

INVESTIGATING THE DRIVERS OF THUCHILA RIVER COURSE ALTERATION IN GROUP VILLAGE HEAD NOGWE, TRADITIONAL AUTHORITY NKANDA, MULANJE DISTRICT, MALAWI

WILBROAD MWASANGWALE, DRM/026/21

THYOLO, MALAWI

DISSERTATION SUBMITTED TO NDATA SCHOOL OF CLIMATE AND EARTH SCIENCES OF THE MALAWI UNIVERSITY OF SCIENCE AND TECHNOLOGY IN PARTIAL FULFILLMENT OF THE REQUIREMENTS FOR THE BACHELOR OF SCIENCE DEGREE IN DISASTER RISK MANAGEMENT

29 MAY, 2026

DISSERTATION APPROVED BY:

SUPERVISOR:

MR. V. KATONDA Signature: 

ASSESSOR: Signature: _____

DISCLAIMER

This document describes work undertaken as part of a programme of study at Ndata School of Climate and Earth Sciences of the Malawi University of Science and Technology. All views and opinions expressed therein remain the sole responsibility of the author(s), and do not necessarily represent those of the school.

COPYRIGHT STATEMENT

This copy of the dissertation has been supplied on condition that anyone who consults it is understood to recognize that its copyright rests with its author and that no quotation from the dissertation and no information derived from it may be published without acknowledgement.

ABSTRACT

This research investigates the physical and spatial impacts of the Thuchila River's course alteration on flood patterns and extent in Group Village Head (GVH) Nogwe, Mulanje District, Malawi. While local flooding is often broadly attributed to extreme weather such as the legacy of Cyclone Freddy and a 129 mm daily rainfall peak in 2025 this study addresses a critical gap in documenting the underlying geomorphological and spatial drivers. Using a quantitative geospatial and hydrodynamic approach, the research integrated Two-Dimensional (2D) HEC-RAS modelling, Remote Sensing, and GIS analysis (p. 20). Longitudinal Land Use and Land Cover (LULC) analysis between 2013 and 2025 revealed a dramatic landscape transformation: settlement areas expanded from 7% (26.1) to 54% (198.7), largely through the conversion of 174.6 of bare land (pp. 31, 33, 36). This aggressive anthropogenic encroachment degraded natural riparian buffers, fundamentally amplifying the region's hazard profile. Hydrological estimations using the Rational Method derived a peak discharge of 191.74 for the 2025 extreme rainfall event was calculated. The 2D hydraulic simulations physically validated the river's avulsion mechanics, mapping new inundation zones with water depths reaching a maximum of 6.39 meters. These modelled outputs, corroborated by field transect walks, demonstrate that the redirected floodwaters now inundate previously safe zones, threatening agricultural livelihoods and causing family displacement. The study concludes that evidence-based land-use planning and community-led resilience strategies are essential to mitigate the heightened flood risks engineered by catchment degradation and climatic variability.

ACKNOWLEDGEMENTS

This work would not have been possible without the guidance, support, and encouragement of several people, to whom I am profoundly grateful.

My deepest appreciation goes to my supervisor, Mr. Vincent Katonda. His invaluable guidance, constructive criticism, and unwavering support were instrumental in shaping this research from its conception to completion.

I extend my thanks to the Malawi University of Science and Technology (MUST) for the opportunity to undertake this study. My gratitude also goes to all the lecturers in the Ndata School of Climate and Earth Sciences for imparting the knowledge that formed the foundation of this work.

To my roommates and dear friends: Khumbo Mayongo, Hope Matemba, Sunday Levi Mmakuwa, and Tamara Chavula, thank you for the constant moral support and encouragement. I am also grateful to my classmates in the final year Disaster Risk Management programme for the shared experiences and camaraderie.

Finally, my profound gratitude goes to my family. Your unconditional love, prayers, and sacrifices have been my greatest source of strength. This achievement is as much yours as it is mine.

Table of Contents

1. CHAPTER ONE: Introduction 1
1.1. Background 1
1.2. Problem Statement 3
1.3. Main Objective 3
1.4. Specific Objective 3
1.5. Research Questions 4
1.6. Significance Of Study 4
2. CHAPTER TWO: Literature Review 5
2.1. Introduction 5
2.2. Conceptual Framework 6
2.3. The Physical Dynamics of River Avulsion and Altered Flood Regimes 7
2.3.1. Geomorphological and Hydrological Drivers of Channel Change 7
2.3.2. Shifting Flood Hazard Zone and Inundation Patterns 7
2.4 Social- Economic Impact of Flooding on Rural Livelihoods 8
2.4.1. Impact On Agricultural Livelihoods 8
2.4.2. Displacement, Social Disruption and Infrastructure Damage 8
2.5. Literature Summary and Research Gap 9
3. CHAPTER THREE: Materials And Methods 11
3.1. Introduction 11
3.2 Description of the Study Area 11
3.3 Research Design 12
3.4 Spatial Data Acquisition and Sources 13
3.5 Land Use and Land Cover (LULC) Change Detection 16
3.6 Catchment Delineation and Hydrological Discharge Estimation 17
3.7 Two-Dimensional (2D) Hydraulic Modelling and Inundation Simulation 18

3.8 Flood Extent Mapping.....19
3.9 Spatial Soil Data Collection and Analysis 20
3.10 Field Validation via Transect Walk.....22
3.11 Data Integration and Analysis.....23
3.12 Ethical Considerations 23
4. CHAPTER FOUR: RESULTS AND DISCUSSION.....25
4.1 Introduction 25
4.2. Results 25
4.3. Discussion 41
4.4. Limitations of the Study.....46
5. CHAPTER FIVE. CONCLUSION AND RECOMMENDATION.....48
5.2 Conclusion.....48
5.1 Recommendations 49
REFERENCES.....51
6. Appendix 57

ACRONYMS/ABBREVIATIONS

DCCMS : Department of Climate Change and Meteorological Services

DRM : Disaster Risk Management

ESA : European Space Agency

GIS : Geographic Information System

GVH : Group Village Headman

HEC-RAS : Hydrologic Engineering Centre's River Analysis System (a software name)

HEVC : Hazard, Exposure, Vulnerability, and Capacity

MUST : Malawi University of Science and Technology

NASA : National Aeronautics and Space Administration

NDVI : Normalized Difference Vegetation Index

PAR : Pressure and Release (Model)

SPSS : Statistical Package for the Social Sciences (a software name)

TA : Traditional Authority

UNDRR : United Nations Office for Disaster Risk Reduction

USA : United States of America

LIST OF FIGURES

Figure 1.1 shows a satellite image of Thuchila river's course in the year 2013 acquired from google earth pro 2
Figure 1.2 shows a satellite image of Thuchila river's course in the year 2024 acquired from google earth pro 2
Figure 2.1 show a causal chain conceptual framework 7
Figure 3.1 shows the study area map of Thuchila catchment area in traditional authority Nkanda in Mulanje 12
Figure 3.2 shows a satellite image extracted from Copernicus hub 13
Figure 3.3 shows a daily precipitation graph from 2013 to 2025 generated from climate engine 15
Figure 3.4 shows an elevation map of the Thuchila catchment area in TA Nkanda 16
Figure 3.5 Shows the soil composition map for the catchment area 21
Figure 3.6 shows the methodological chart used in this research 24
Figure 4.1 shows the natural colour composite of Thuchila catchment in a for the year 2013 26
Figure 4.2 shows a natural colour composite for traditional authority Nkanda for the 2025 imagery 27
Figure 4.3 shows the land use land cover classification map for 2013 Landsat imagery for 2013 28
Figure 4.4 shows a pie chart that represent the area of class names in percentage 29
Figure 4.5 shows a land use and land cover map for 2025 sentinel-2 imagery 30
Figure 4.6 shows a pie chart that represent the area of a given class in percentage 31
Figure 4.7 shows a change detection map for 2013 to 2025 satellite imagery 32
Figure 4.8 shows a graph for area change during change detection analysis 34
Figure 4.9 Shows velocity of flood water and some affected villages 36
Figure 4.10 shows depth of flooding water during 2D simulation 37
Figure 4.11 shows water surface elevation (WSE) generated during 2D HEC-RAS simulation 38
Figure 4.12 shows the satellite image of the study area and area occupied by water during 2D simulation 39
Figure 4.13 shows a hydrograph of velocity with time at a certain point on the flooding area 40
Figure 4.14 shows a hydrograph of depth with time at a certain point on the flooding area 41
Figure 4.15 shows the old and current river channel of Thuchila river 43
Figure 6.1 shows silted Thuchila river 57
Figure 6.2 shows eroded Thuchila river banks 57
Figure 6.3 shows rocked in the upper side of the river that were transported by the river waters 58

Figure 6.4 shows flooded water after water overtopping the banks..... 59
Figure 6.5 shows the borehole underwater after river flooding 60

LIST OF TABLES

Table 2.1 shows a Causal Chain of Flood Risk in GVH Nogwe following the Thuchila River Avulsion 9
Table 4.1 shows area calculated from each class name after supervised classification . 28
Table 4.2 shows the area occupied by a given class after supervised classification of 2025 imagery 31
Table 4.4 shows area that have been converted into other classes after a change detection map 33
Table 4.5 shows the accuracy assessment for a 2013 supervised classification map 35
Table 4.6 shows accuracy assessment of a 2025 supervised classification map 35

1. CHAPTER ONE: Introduction

1.1. Background

Flooding is defined as the overflow of water onto land that is normally dry, often triggered by heavy rainfall, river overflow, or cyclonic activity (UNDRR, 2021). It is one of the most frequent and damaging natural hazards globally, accounting for nearly half of all recorded disasters and affecting over 2.3 billion people in the past two decades (Suhr & Steinert, J. I., 2022). Floods have intensified in Sub-Saharan Africa due to climate variability, land use transformation, and accelerated urban growth, with rural communities and medium-sized towns being subjected more (Enua et al., 2024).

Malawi, in particular southern regions, are perpetually hit by floods that have a risk to lives, livelihoods, development achievement and cause rivers to breach. Mulanje District has fertile soils and agricultural output, where maize, rice, sorghum, and pigeon peas are the dominant local livelihood crops. However, the district's terrain and rainy conditions with seasonal patterns make it highly susceptible to flooding (Nangoma & Everhart , 2008). In the recent decades, river course alteration has exacerbated flood impacts, drawing water into what was previously less affected regions and increasing frequency and intensity (Vakhani, 2024). The villages of Group Village Headman (GVH) Nogwe, villages of Sadibwa, Katuma, and Mbunumbu are specifically seriously affected, as they lie within areas prone to flooding along the Thuchila River in Mulanje district which is changing its course.

Forest clearing, land use change, and agricultural encroachment have reduced natural buffers and increased runoff, and river diversion has forced floodwaters into vulnerable areas (Prabal et al., 2019).. These changes endanger subsistence farming societies, reducing arable land, contaminating water sources, and resulting in epidemics of waterborne diseases. During my field experience with the Mulanje District Council, I conducted field surveys and witnessed firsthand the impacts in Sadibwa, Mbunumbu, and Katuma. Already two weeks before Cyclone Jude, individuals had already been displaced from their homes in GVH Nogwe due to flooding; the cyclone further worsened the situation, dislocating families into emergency camps.



Figure 1.1 shows a satellite image of Thuchila river's course in the year 2013 acquired from google earth pro



Figure 1.2 shows a satellite image of Thuchila river's course in the year 2024 acquired from google earth pro

This study analyses the drivers of Thuchila River course alteration and avulsion in GVH Nogwe. It aims to assess the causes and determine the extent of flooding through simulation, find mitigation strategies, and recommend feasible, community-based solutions to enhance resilience. In accordance with the Sendai Framework for Disaster Risk Reduction (2015–2030), the study contributes to increased disaster risk awareness, locally led approaches, and sustainable planning in Mulanje District.

1.2. Problem Statement

The Thuchila River has recently undergone a catastrophic course alteration, broken its historical banks and forged a new path through GVH Nogwe. While this disaster is often broadly attributed to recent extreme weather events, such as the 129 mm daily rainfall peak in 2025 and the legacy of Cyclone Freddy, the underlying spatial and geomorphological drivers remain undocumented. Without empirical data, disaster management authorities are operating blindly. There is a critical lack of precise spatial quantification regarding how much land degradation has occurred over the last decade, and no hydrodynamic models exist to map the true multi-directional extent of the floodwaters under extreme discharge scenarios. This study addresses this gap by deploying Remote Sensing, hydrological calculations, and Two-Dimensional (2D) HEC-RAS modelling to physically map the avulsion and quantify the specific land-use changes (from 2013 to 2025) that engineered the disaster in GVH Nogwe.

1.3. Main Objective

The main objective of this study is to investigate the hydrodynamic and geomorphological drivers of the Thuchila River course alteration in GVH Nogwe.

1.4. Specific Objective

a) To assess the spatial and temporal Land Use and Land Cover (LULC) changes in the Thuchila River catchment between 2013 and 2025 using optical satellite imagery.
b) To estimate the peak hydrological discharge of the Thuchila River during extreme precipitation events utilizing the empirical Rational Method.

c) To model the multi-directional flood inundation extent and study physical avulsion mechanics.

1.5. Research Questions

a) What were the predominant Land Use and Land Cover (LULC) transitions within the Thuchila catchment between 2013 and 2025?
b) What was the estimated peak discharge volume generated by the extreme localized rainfall events?
c) How does the 2D modelled flood extent align with the newly encroached settlement zones in GVH Nogwe?

1.6. Significance Of Study

This study is its capacity to address one of the largest issues that has been plaguing Mulanje District communities flooding and livelihoods. By examining the changed river courses and emerging flood patterns, the research presents deep insight into how environmental change, land use and climate variability are re-shaping the environment and rural livelihood (Nile et al., 2025).

The study is particularly useful for application in setting local and district policy, making evidence-based suggestions that can be used to guide disaster preparation, land use planning, and infrastructure development (Fitriyati et al., 2024). The study also contributes to academic literature by closing a gap in localized studies on hydrological changes and community exposure in the southern part of Malawi. Furthermore, the study empowers vulnerable communities by amplifying their voice and presenting feasible, locally suitable solutions to minimize flood risk (Kundzewicz et al., 2014). For this purpose, it supports inclusive development and resilience approaches to ensure that not only technically good interventions but also socially just and sustainable ones are actually implemented (Majlingova & Kadar, 2025).

2. CHAPTER TWO: Literature Review

2.1. Introduction

Rivers across the globe periodically and sometimes catastrophically changed course, a process referred to as river avulsion, re-sculpting landscapes and communities. Historical records show that avulsions on China's Yellow River in the late 19th and early 20th centuries caused floods that killed over six million people, while similar events along the Tigris and Euphrates rivers contributed to the decline of ancient Mesopotamian civilizations (Ganti, 2022).

Satellite images have documented more than 100 avulsion events worldwide for 50 years ago in diverse climates and geomorphic settings, from the Mississippi delta in the USA to the Kosi River in India that in 2008 meandered over 100 kilometers within a few days, rendering more than three million individuals homeless (Ganti, 2022). They are typically caused by sedimentation that raises the riverbed and makes water seek a lower channel, and are becoming more defined through climate change, land-use pressure, and catchment degradation (Gearon et al., 2024).

Among the most prevalent and destructive natural hazards in Malawi is flooding, and southern areas such as Mulanje have experienced repeated episodes due to their geographical location and geomorphology, intensity of rainfall, and deforestation. (Government of Malawi et al., 2019). Chauluka, Singh, and Kumar (2021) carried out a long-term examination of rainfall and streamflow patterns in the Thuchila River catchment from 1985 to 2016. Applying Mann–Kendall and Pettitt tests, they identified non-significant but apparent declining trends in annual and seasonal rainfall, accompanied by erratic streamflow patterns with slight increases in wet-season flows and decreases in dry-season flows (Chauluka et al., 2021). They found change points in the mid-2000s as well, which coincided with record-breaking weather events that altered rainfall–runoff relations. Their research is helpful as a hydro-climatic baseline to inform how Cyclone from 2019 to 2025 impacts on increasing the streamflow of the Thuchila river which led to the shift in the river's course to be differ from historical patterns and increase flood risk in GVH Nogwe.

In Malawi, cases of catastrophic weather such as Cyclone Freddy (2023) have indicated that avulsion is not merely a global issue but also a local hazard with significant effects on disaster risk management. In group village head Nogwe, traditional authority Nkanda, the dramatic course change of the Thuchila River redirected classic flood patterns, inundating previously unswollen areas and disrupting livelihood. Understanding the relationship between hydrological and hydraulic processes, geomorphological alteration, land-use change, and climate fluctuation is essential for developing effective, evidence-based responses (Dwarakish & Ganasri, 2015).

2.2. Conceptual Framework

The HEVC model separates the risk of flooding into four components: hazard (the altered river course and flood regime), exposure (settlements and assets in flood-risk zones), vulnerability (weak infrastructure and vulnerable livelihoods), and capacity (local coping mechanisms and institutional support). By assessing these components, the research will generate composite risk maps showing locations most high velocity which is ideal to cause erosion and deposition of sediments.

The pressure and release (PAR) model build on this by unpacking the root drivers of vulnerability. It identifies root causes such as deforestation and absence of land-use enforcement, dynamic pressures such as encroachment of agriculture and settlement expansion, and unsafe conditions such as poor drainage and degraded vegetation (Wisner et al., 2004). Together, the models provide a comprehensive picture of flood risk and guide the development of actionable, locally tailored solutions. The PAR framework is underpinned by fluvial geomorphology theory, which explains how river channel form responds to sediment load, discharge, and bank stability (Knighton, 2014).

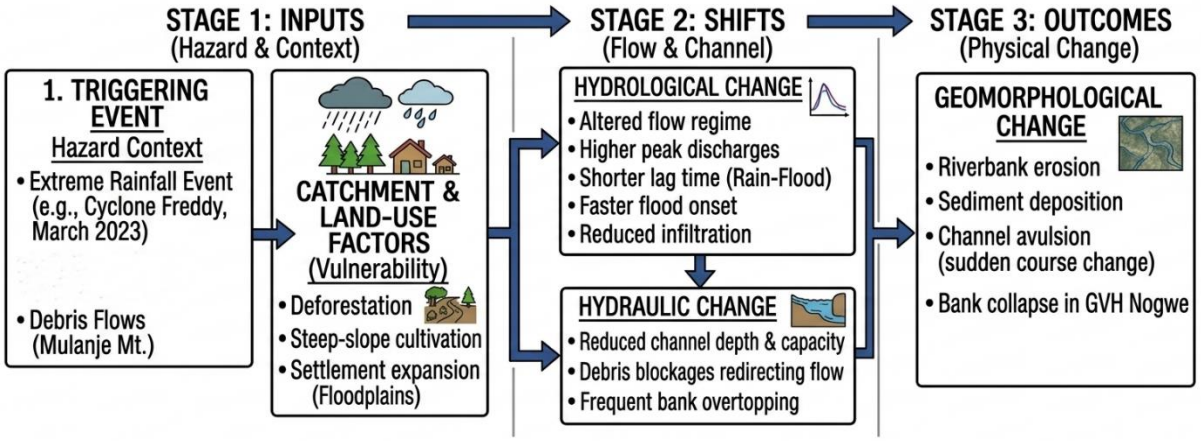


Figure 2.1 show a causal chain conceptual framework

2.3. The Physical Dynamics of River Avulsion and Altered Flood Regimes

2.3.1. Geomorphological and Hydrological Drivers of Channel Change

Avulsion of channels occurs when cyclone-driven flooding causes rivers to leave their traditional channel for an alternative path, often due to bank erosion, sedimentation, or debris jamming (Slingerland & Smith, 2004). Concentrated rainfall in mountainous catchments results in accelerated sediment transportation, and this results in alterations in channel cross-sections as well as a reduction in the conveyance capacity (Simon & Rinaldi, 2013). Hydrological changes include increased peak discharges and reduced lag times between the rainfall and flood peaks, caused by catchment degradation and degradation of infiltration capacity increase the risk of flooding since stream will be carrying more water than its capacity with an increase in run-off water (Juan-Diego et al., 2025). Hydraulic changes such as reduced channel depth and altered flow velocities are often supplemented by debris jams that divert flows into settlements (Petts & Gurnell, 2005). Mozambican research after Cyclone Idai (2019) presents concurrent trends, with geomorphological instability amplifying the impacts of floods, mirroring trends observed in southern part of Malawi (World Bank, 2019).

2.3.2. Shifting Flood Hazard Zone and Inundation Patterns

Change in morphology can significantly shift flood hazard zones, increasing exposure in what were previously considered safe zones. In Malawi's Lower Shire, river avulsions

have been linked to new floodplain inundation patterns, with increased flood frequency even under moderate rainfall (Mlera & Chavula, 2016). The altered Thuchila River course likely reduced channel capacity in some reaches while creating new flow paths, leading to deeper and longer-lasting inundation in low-lying areas. Southern Malawi climate change projections indicate a rise in the intensity of rainfall events, which, combined with altered channel geometry, may enhance flood risk (Douville et al., 2021). Remote sensing and GIS-based flood modeling have been utilized already in similar circumstances to map areas affected by post-avulsion floods and guide relocation planning (Di Baldassarre et al., 2010).

2.4 Social- Economic Impact of Flooding on Rural Livelihoods

2.4.1. Impact On Agricultural Livelihoods

Agriculture is most often the major source of food and income in rural areas. During floods, they destroy crops, sweep away seed stocks, and leave behind sand and trash on terrain which can no longer be used in the future for cultivation. Armah et al. (2010) noted in Northern Ghana that over 70,000 hectares of agricultural land had been flooded, leading to massive food shortages and loss of earnings. In Malawi, the same impact is also experienced especially in districts that experience flooding like Chikwawa, Nsanje, and Mulanje districts where farmers may lose one season's harvest and only recover years later (Di Baldassarre et al., 2010).

2.4.2. Displacement, Social Disruption and Infrastructure Damage

Flooding displaces people from their homes and forces them to relocate to temporary camps or safe grounds. This displacement interferes with their access to land, markets, and social networks. When people move, they abandon their farms, livelihoods, and social networks making it harder to begin their lives again. Relief camps are usually overcrowded and lack proper sanitation, thereby increasing the danger of diseases and reducing productivity. Armah et al. (2010) further observed that when societies are severely affected, even strong social networks are strained (Armah et al., 2010). Floods not only damage homes and cropland they can ruin roads, bridges, and marketplaces. This prevents farmers from reaching market, obtaining inputs, or seeing a doctor. For instance, Following Cyclone Idai it reported destroyed infrastructure in Mozambique

cut off many communities from access for weeks, worsening food insecurity and hampering recovery. The same issues happen in Malawi when floods destroy major roads, isolating villages and halting business (World Bank, 2019).

2.5. Literature Summary and Research Gap

Literature examined points out that river course change following episodes of intense weather is both a geomorphological and socio-economic process. Cyclone Freddy's impact on the Thuchila River is in line with worldwide evidence that avulsion events can change flood hazard zones extremely rapidly, increasing exposure and vulnerability. Hydrological and hydraulic changes caused by catchment degradation, climatic variability, and land-use pressure increase the threat (Setti et al., 2024). Livelihood impacts are multifaceted, with influences on agriculture, housing, health, and market access. The PAR model provides a useful framework to link physical processes to vulnerability, while fluvial geomorphology can contribute to understanding mechanisms of channel change. Flood dynamics following avulsion in Malawi have a lack of empirical work conducted on them, indicating a gap this paper aims to fill.

Table 2.1 shows a Causal Chain of Flood Risk in GVH Nogwe following the Thuchila River Avulsion

Stages	Description	Evidence/Examples	Link to Research Objectives
1. Triggering Event	Extreme rainfall and strong Cyclone (e.g., Freddy in March 2023)	>500 mm rainfall in 72 hours; debris flows from Mulanje Mountain slopes	Sets the hazard context for Objective 2
Catchment & Land-Use Factors	Deforestation, cultivation on steep slopes, and settlement	Loss of riparian vegetation; increased surface runoff; unstable riverbanks	Objective 1

	expansion into floodplains		
Geomorphological Change	Riverbank erosion, sediment deposition, and channel avulsion (sudden change in river course)	Thuchila River diverted into new channel sections; bank collapse in GVH Nogwe	Objective 3: Analyses geomorphological changes
Hydrological Change	Altered flow regime: higher peak discharges, shorter lag time between rainfall and flooding	Faster flood onset; reduced infiltration due to degraded catchment	Objective 2, estimating peak discharge during extreme rainfall
Hydraulic Change	Reduced channel depth and capacity; debris blockages redirecting flow	Floodwaters overtopping banks more frequently	Objective 3, hydraulic modelling
Altered Flood Patterns	New inundation zones, increased flood frequency, greater depth and duration	Previously safe areas now flood-prone; prolonged waterlogging	Objective 2: Assess changes in flood patterns
Livelihood Impacts	Damage to crops, homes, infrastructure; loss of income; displacement; health risks	Sand deposition on fields; road/bridge damage; cholera outbreaks in camps	Objective 2: Evaluate impacts on livelihoods

3. CHAPTER THREE: Materials And Methods

3.1. Introduction

This chapter outlines the research methodology employed to investigate the physical and spatial causes of the Thuchila River's course alteration within Group Village Head (GVH) Nogwe. It details the research design, data acquisition techniques, analytical tools, and field validation methods that guided the study. A quantitative geospatial and hydrodynamic modelling approach was adopted, integrating Remote Sensing, Hydrology, and Two-Dimensional (2D) HEC-RAS simulations supplemented by qualitative field observations to provide a holistic, ground-trothed understanding of the avulsion and subsequent flood extent.

3.2 Description of the Study Area

The study is localized in Group Village Head (GVH) Nogwe, within Traditional Authority (T/A) Nkanda in Malawi's Mulanje District, focusing specifically on the 366.9-square-kilometer Thuchila River catchment. Topographically, the river descends from the steep, high-altitude terrain of the Mulanje Massif into the flat, low-lying floodplain of GVH Nogwe. This abrupt transition from high to low gradients rapidly decreases flow velocity, driving heavy sediment deposition. Consequently, the natural geomorphology makes the local riverbanks highly susceptible to lateral erosion, meandering, and the avulsion events central to this research.

Climatically, the region experiences a tropical savanna climate driven by the Inter-Tropical Convergence Zone and cyclonic systems. These torrential rains generate massive runoff from the massif, periodically overwhelming channel capacities. Compounding this physical vulnerability is the area's socio-economic reliance on rural agriculture. Over the 12-year study period (2013-2025), aggressive anthropogenic encroachment systematically converted bare land into settlements and agricultural plots. This rapid expansion severely degraded the protective riparian buffer, fundamentally amplifying the spatial hazard profile of the GVH Nogwe community

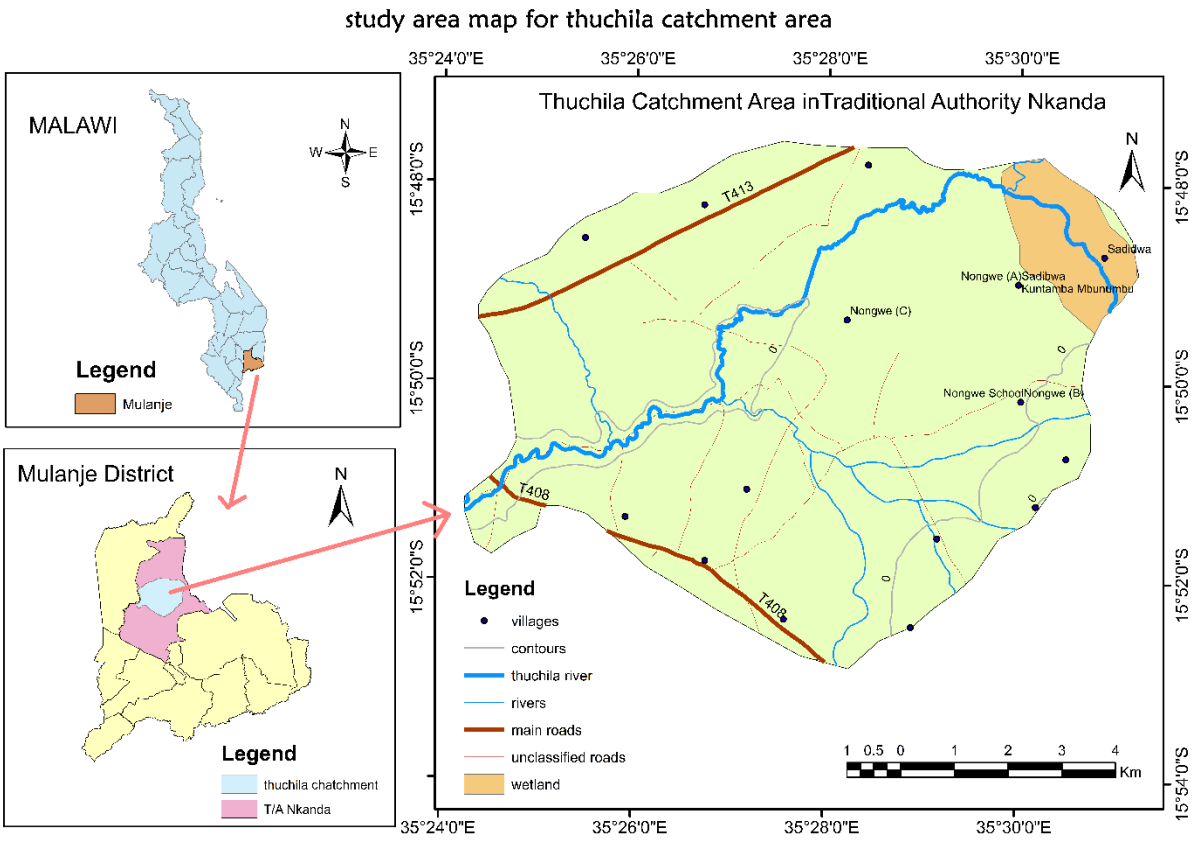


Figure 3.1 shows the study area map of Thuchila catchment area in traditional authority Nkanda in Mulanje

3.3 Research Design

The study utilized a geospatial and physical science research design, prioritizing spatial modelling and hydraulic simulation to quantify the disaster risk landscape. This approach allowed for the empirical mapping of the river's avulsion, historical land use changes, and multidirectional hydraulic inundation capacities. To validate the digital models against real-world conditions, an observational field-validation strategy was employed. The integration of digital modelling and physical ground-truthing ensured high accuracy in delineating the actual flood extent and understanding the physical environmental pressures driving the disaster.

3.4 Spatial Data Acquisition and Sources

To investigate the physical changes in the Thuchila River catchment, a combination of remote sensing imagery, hydro-meteorological data, spatial soil data and topographical data was acquired:

3.3.1 Satellite Imagery

To establish a longitudinal visual record of land cover alteration and river avulsion, optical satellite imagery was utilized. Baseline pre-diversion imagery was sourced from the Landsat satellite program for the year 2013. To capture the current, post-diversion landscape, high-resolution Sentinel-2 imagery was acquired for the year 2025.

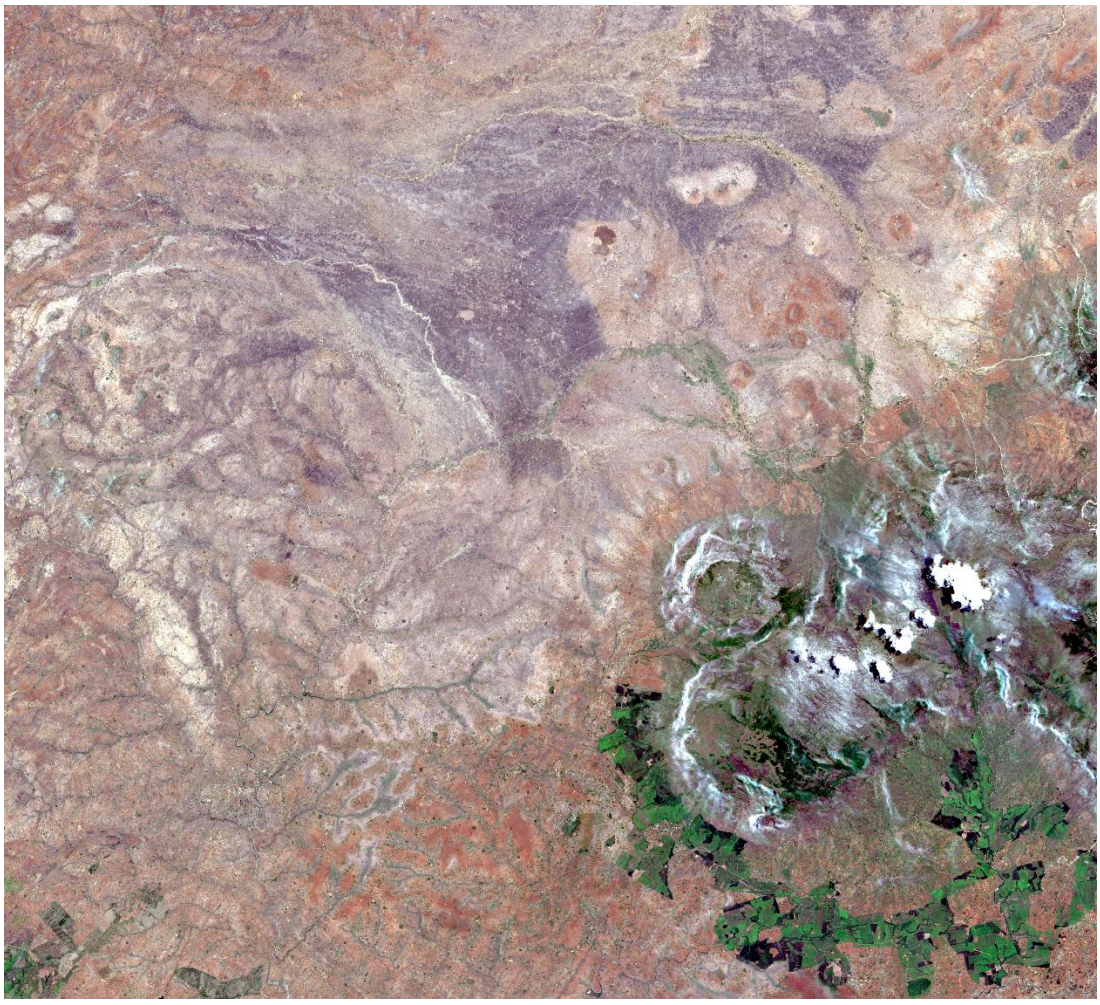


Figure 3.2 shows a satellite image extracted from Copernicus hub

3.3.2 Precipitation Data

To evaluate historical and contemporary precipitation trends between 2013 and 2025, this study utilized the CHIRPS (Climate Hazards Group InfraRed Precipitation with Station data) dataset. Accessed via the Climate Engine platform, the data was extracted strictly as a time-series to analyze temporal rainfall patterns without the need for supplementary local ground gauges. The extracted data was organized into two distinct formats: a tabular Excel spreadsheet for quantitative analysis and a hydrograph for visual temporal tracking. This dual-format approach was instrumental in pinpointing specific extreme weather anomalies. By analyzing the peaks in the hydrograph alongside the exact figures in the dataset, the study was able to clearly isolate and quantify the severe rainfall intensity of the area, as well as the extreme precipitation spikes recorded severe rainfall intensity of the area, as well as the extreme precipitation spikes recorded.

The dataset was extracted using a single coordinate located at the geographic center (centroid) of the 366.9 km² catchment area. Given CHIRPS's spatial resolution of 0.05° (approximately 30.25 km² per data pixel), this methodology utilizes the central pixel as a representative index for the broader catchment. The primary implication of this point-based extraction is that it operates on the assumption of spatial uniformity across the study area. While this approach may not capture isolated, highly localized convective storms at the catchment's extreme boundaries, it is highly robust for assessing massive, synoptic-scale weather systems. Because the 2013–2025 study period was characterized by multiple large-scale cyclonic systems and widespread extreme weather events, these massive storms effectively blanketed the entire region. Therefore, the central extraction point serves as an accurate and mathematically sound proxy for evaluating the severe rainfall intensities experienced by the catchment as a whole during these major climatic anomalies.

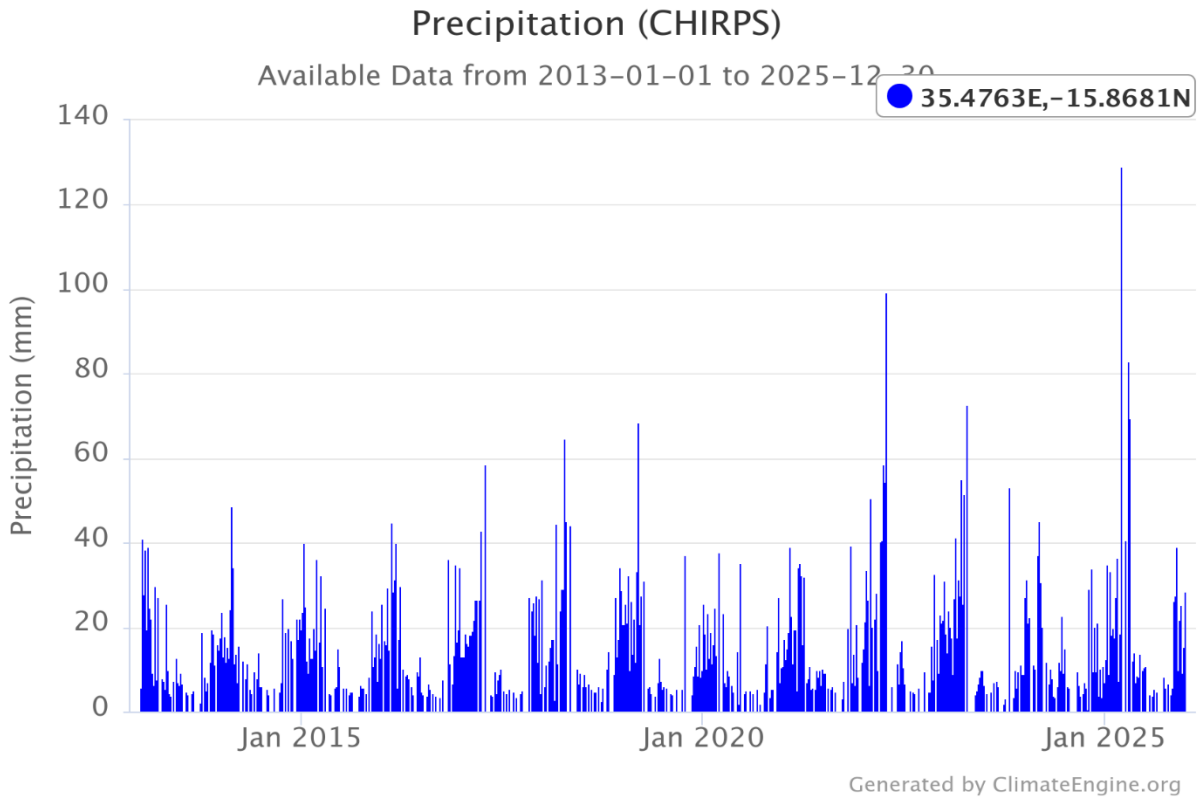


Figure 3.3 shows a daily precipitation graph from 2013 to 2025 generated from climate engine

3.3.3 Topographical Data

Digital Elevation Model (DEM) was acquired from the United States Geological Survey (USGS), utilizing the 30-meter resolution Shuttle Radar Topography Mission (SRTM) dataset to analyze the physical slope, channel geometry, and structural boundaries of the catchment.

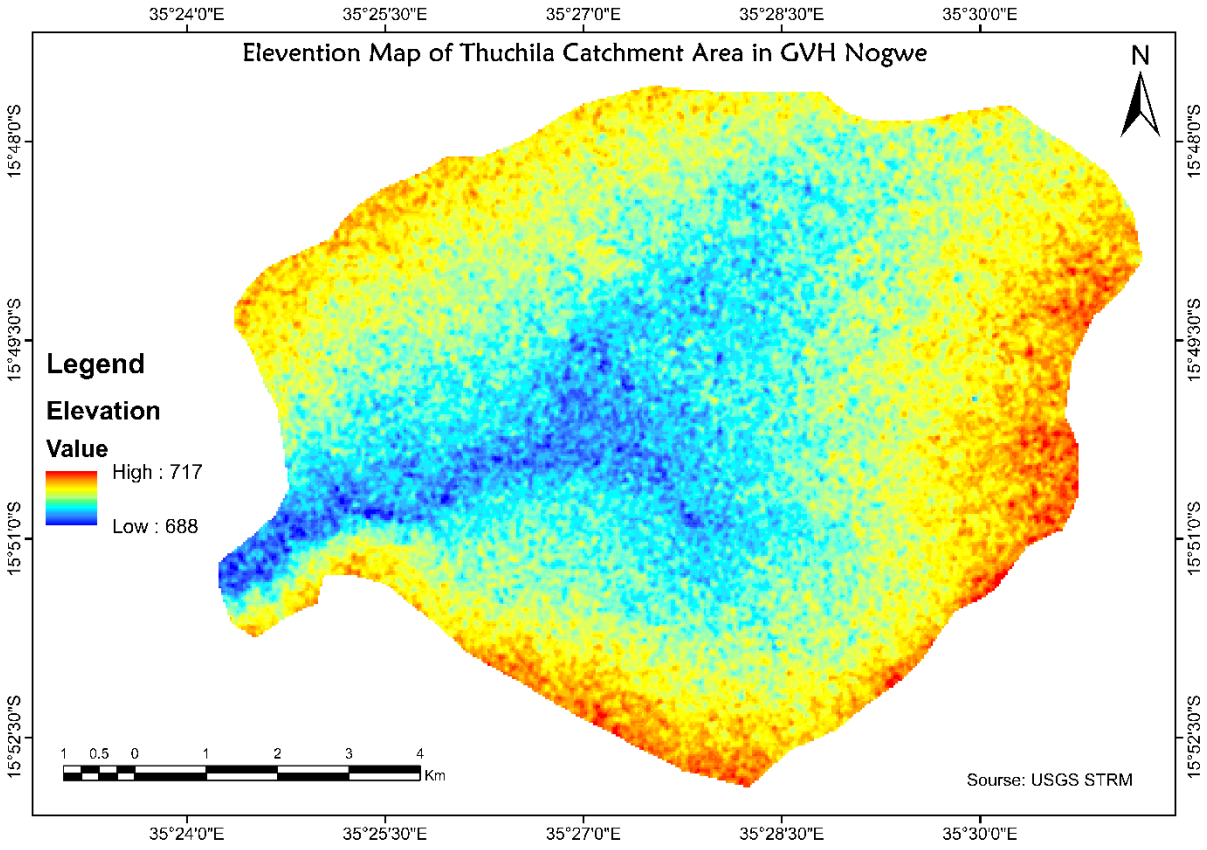


Figure 3.4 shows an elevation map of the Thuchila catchment area in TA Nkanda

3.5 Land Use and Land Cover (LULC) Change Detection

To quantify the anthropogenic impacts on the catchment that contributed to the river's diversion, a Land Use and Land Cover (LULC) classification and change detection analysis was conducted within a Geographic Information Systems (GIS) environment.

The landscape was categorized into three primary LULC classes:

1. Bare Land, land without vegetation, can be unbuilt or agricultural land
2. Settlement, usually built land
3. Vegetation, land with trees

Supervised classification techniques were applied to both the 2013 Landsat and 2025 Sentinel-2 imagery to extract the total area for each class per year. Subsequently, a post-classification change detection transition matrix was generated to calculate the spatial

shifts between classes over the 12-year period. This matrix explicitly quantified critical environmental degradation, notably highlighting the extensive conversion of bare land into human settlements, providing empirical spatial evidence of increased human encroachment within the flood-prone zones.

3.4.1 Classification Accuracy Assessment

To ensure the scientific validity and reliability of the LULC maps, a rigorous accuracy assessment was conducted on the supervised classification outputs. A stratified random sampling method was employed to generate validation points across the classified maps. These points were then cross-referenced against high-resolution reference imagery and historical ground-truth data to verify the true land cover class. A confusion matrix was computed to evaluate classification performance, allowing for the calculation of Overall Accuracy, Producer's Accuracy, and User's Accuracy. The Kappa coefficient was also derived to measure the agreement between the classified map and the ground reference data, ensuring that the identified land use transitions were statistically robust.

3.6 Catchment Delineation and Hydrological Discharge Estimation

To assess the hydrological response of the Thuchila River to observed precipitation extremes, it was necessary to calculate peak surface runoff. First, the DEM was projected to the UTM Zone 36S coordinate reference system to accurately delineate the specific contributing boundaries of the Thuchila catchment, yielding a calculated basin area of 366.9 square kilometers.

To estimate the peak river discharge resulting from extreme weather, the empirical Rational Method formula was deployed (Mostrales et al., 2018)

$$Q = \frac{(C \times P \times A)}{T}$$

Where:

- Q = Discharge flow rate (in cubic meters per second, m3/s)
- C = Runoff Coefficient
- P = Precipitation (Rainfall depth, converted to meters)
- A = Catchment Area (converted to square meters)
- T = Time duration (in seconds)

The variables were applied as follows:

- A standard runoff coefficient (C) of 0.35 was applied, representing the mixed agricultural, settlement, and hilly terrain characteristic of the catchment.
- The peak daily precipitation (P) of 129.004 mm (0.129004 meters), identified via the Climate Engine dataset for 2025, was utilized to calculate the total rainfall volume over the catchment area (A).
- Distributing this runoff volume over a 24-hour temporal baseline (T = 86,400 seconds) yielded an estimated average continuous discharge flow (Q) of 191.74 cubic meters per second (m^3/s).

3.7 Two-Dimensional (2D) Hydraulic Modelling and Inundation Simulation

To simulate the complex, multi-directional physical behaviour of the floodwaters and understand the exact hydraulic mechanics behind the river's avulsion into GVH Nogwe, two-dimensional (2D) hydrodynamic modelling was conducted using the Hydrologic Engineering Centre's River Analysis System (HEC-RAS). Unlike traditional 1D modelling, which confines flow to linear cross-sections, the 2D approach allows for the dynamic routing of water longitudinally and laterally across the floodplain.

3.6.1 Terrain Processing and 2D Mesh Generation

The 30m resolution DEM was imported into HEC-RAS Mapper to serve as the foundational terrain model. A 2D Flow Area was defined, encompassing the primary Thuchila River channel, the historical avulsion pathways, and the adjacent vulnerable settlements. A detailed computational mesh was generated across this spatial boundary,

allowing the software to calculate water depth, velocity, and multi-directional movement across every individual grid cell of the landscape.

3.6.2 Boundary Conditions and Flow Routing

To run the 2D hydraulic simulation, the estimated peak discharge calculated via the Rational Method was utilized. An inflow hydrograph featuring the steady peak flow rate of 191.74 m^3/s was applied at the upstream boundary condition of the 2D Flow Area. Normal depth boundary conditions were established at the downstream exit to allow the software to accurately compute the energy grade line and water surface elevations as the flood wave propagated through the mesh.

3.6.3 2D Output Generation and Spatial Correlation

The 2D simulation generated comprehensive hydrodynamic parameters across the study area. The model successfully produced detailed spatial outputs, including continuous Water Surface Elevation maps, Depth profiles, and Flow Velocity vectors that physically demonstrated the lateral spreading of the floodwaters. These 2D outputs allowed for the precise identification of channel breakout points, physically validating how the floodwaters escaped the main channel and inundated the specific settlement zones identified in the LULC spatial analysis.

3.8 Flood Extent Mapping

To translate the hydraulic model into a usable disaster risk product, a Flood Extent Map was generated. The multi-directional water surface elevations calculated during the 191.74 m^3/s 2D simulation were spatially interpolated and overlaid onto the DEM and the 2025 Sentinel-2 imagery. By mapping where the simulated water levels exceeded the surrounding terrain elevation, a definitive inundation boundary (flood footprint) was delineated. This flood extent layer was then cross-referenced with the LULC settlement class to visually quantify the specific inhabited areas of GVH Nogwe that fall within the active hazard zone.

3.9 Spatial Soil Data Collection and Analysis

To understand how the landscape and soil in the Thuchila River catchment and GVH Nogwe floodplain react to flooding, spatial soil data was collected from the Soil and Terrain (SOTER) database for Malawi (2016). This data was loaded into a Geographic Information System (GIS) environment. Software tools were then used to crop (clip) the data so it only showed the specific boundaries of the study area, creating a customized soil composition map.

Next, the map's data tables were analysed to identify the main soil types that affect water flow and soil movement in the catchment. The analysis showed a clear geographic shift. in the south west East, the area is covered by gravel, easily eroded soils (Manganiferric Skeletic Lixisols). During heavy rainfall, high-velocity surface water flows from the North East down towards the South West, carrying large amounts of eroded dirt and gravel. This material is then deposited into the lower, flat floodplain in the South West, which is made up of loose, river-deposited soils (various types of Cambisols). These specific soil types were examined to find their natural weaknesses when exposed to heavy rainfall and flooding. The study looked at key features like how the floodplain soils shrink and crack when dry and swell when wet, how their natural salts dissolve in water, and how easily the topsoil breaks apart.

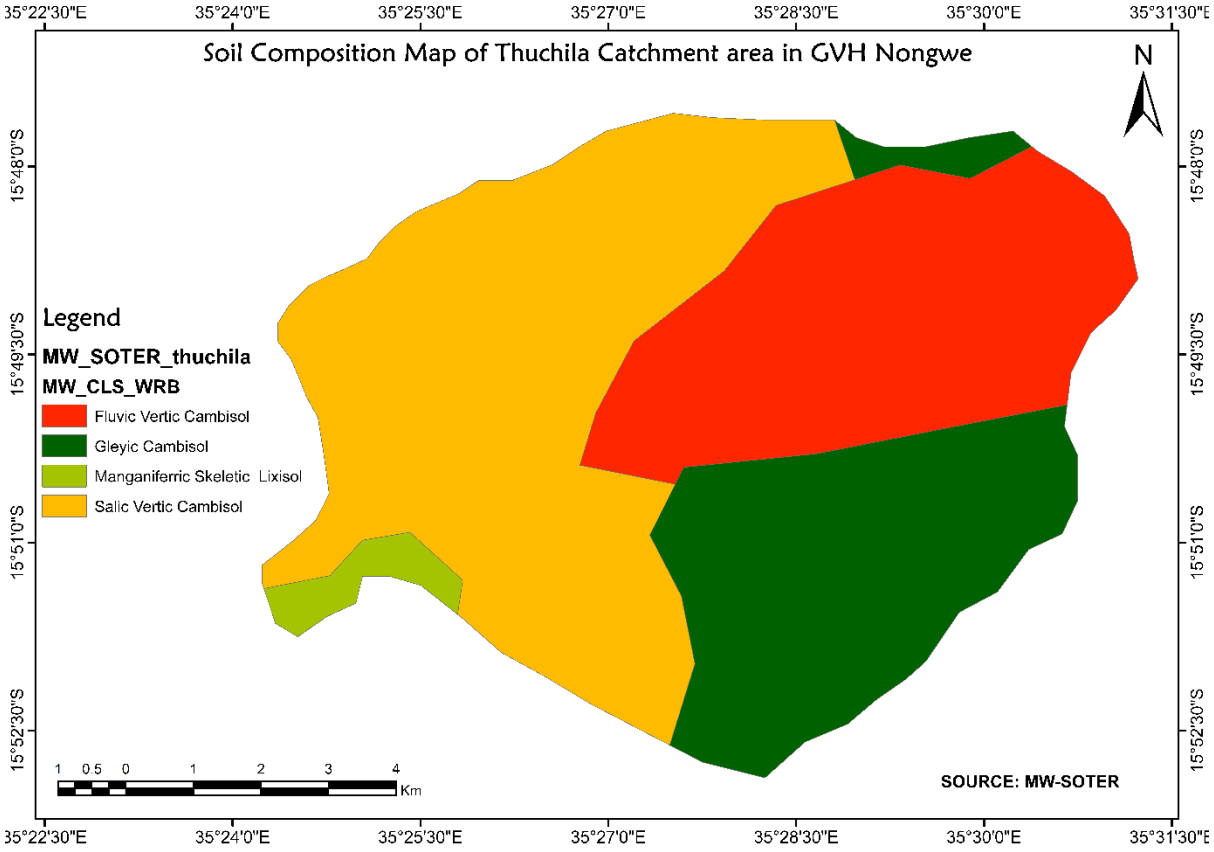


Figure 3.5 Shows the soil composition map for the catchment area

Lixisols are highly weathered tropical and subtropical soils developed over long periods with alternating wet and dry seasons. Structurally, they are defined by the downward leaching of fine clay particles from the surface layer into a deeper, clay-rich accumulation zone known as an argic subsurface horizon. Chemically, they maintain a high base saturation, meaning they actively retain important plant nutrients like calcium, magnesium, and potassium at neutral to slightly acidic pH levels (Morgan, 2005). However, because their clay mineralogy consists primarily of low-activity clays like kaolinite, they possess low moisture-retention capacities. Physically, their topsoils suffer from weak aggregate stability and low organic matter content, which causes the surface to collapse and "slake" under heavy rain, forming a hard, impermeable crust that makes them highly prone to severe sheet and rill erosion if the natural vegetation cover is cleared (Jones et al., 2013).

Cambisols are structurally young, moderately developed soils representing an early, transitional stage of soil formation that occurs widely across global landscapes. Instead

of showing advanced weathering or heavy clay migration, they feature a cambic subsurface horizon characterized by subtle changes in color, structure, or minor mineral alteration compared to the raw underlying parent material. Because they are relatively young and have not been subjected to prolonged leaching, Cambisols naturally exhibit high chemical fertility, a favorable nutrient status, and a rich assembly of weatherable minerals that continuously release nutrients into the soil matrix. Physically, they are characterized by excellent aggregate stability, a highly workable and porous structure, and a variable texture ranging from loamy sands to heavy clays that depends entirely on the local bedrock or alluvial river deposits from which they originated (Morgan, 2005).

Gleyic soils (or Gleysols) are defined entirely by the permanent, dominant influence of groundwater saturation and waterlogging, typically forming in low-lying topographic depressions, flat floodplains, or areas with shallow water tables. Continuous water saturation depletes all soil oxygen, creating an anaerobic, reducing environment that forces soil microbes to use iron and manganese compounds for respiration. This chemical process reduces ferric iron (which is red/brown) into soluble ferrous iron, creating a characteristic greyish-blue or greenish soil matrix known as gleying, punctuated by bright orange or yellow iron mottles where oxygen occasionally penetrates along seasonal water table cracks. Physically, because they sit in saturated sink zones, gleyic soils possess exceptionally poor internal drainage and low hydraulic conductivity. When completely saturated, the soil matrix loses its cohesive shear strength, becoming highly unstable and prone to structural collapse or liquefaction under physical pressure (Jones et al., 2013).

3.10 Field Validation via Transect Walk

To physically validate the outputs of the spatial and hydrodynamic models, primary observational fieldwork was conducted using a transect walk. A planned route was mapped through GVH Nogwe, intersecting the old river channel, the newly avulsed

channel, and the areas identified as highly vulnerable in the LULC and flood extent maps. During the walk, direct observations were recorded regarding:

- The physical state of the avulsed riverbanks and active erosion sites.
- Visual confirmation of land degradation, bare soil, and recent settlement encroachment.
- High-water levels were observed on 21 march 2026 and physical remnants of recent flood damage to corroborate the simulated HEC-RAS water depth simulation.

This ground-truthing exercise ensured that the remote sensing and mathematical modelling accurately reflected the real-world geomorphological realities of the Thuchila River.

3.11 Data Integration and Analysis

The final analytical phase involved triangulating the digital data with the physical field observations. The spatial outputs from the LULC change detection (showing increased settlement in bare lands), the multi-directional 2D HEC-RAS inundation boundaries (defining the flood extent), and the visual evidence gathered from the transect walk were synthesized. This integration provided a comprehensive, evidence-based explanation of how the physical alteration of the river course, combined with extreme rainfall and land use changes, has physically shaped the current flood disaster in GVH Nogwe.

3.12 Ethical Considerations

The research adhered to strict academic and ethical protocols mandated by the Malawi University of Science and Technology (MUST). Prior to conducting the field transect walk, clearance was obtained from local authorities, including the Traditional Authority Nkanda and GVH Nogwe. The fieldwork was strictly observational, focusing on the physical environment and landscape topography, thereby minimizing intrusion into the private lives of the local residents while ensuring the study was conducted respectfully and transparently.

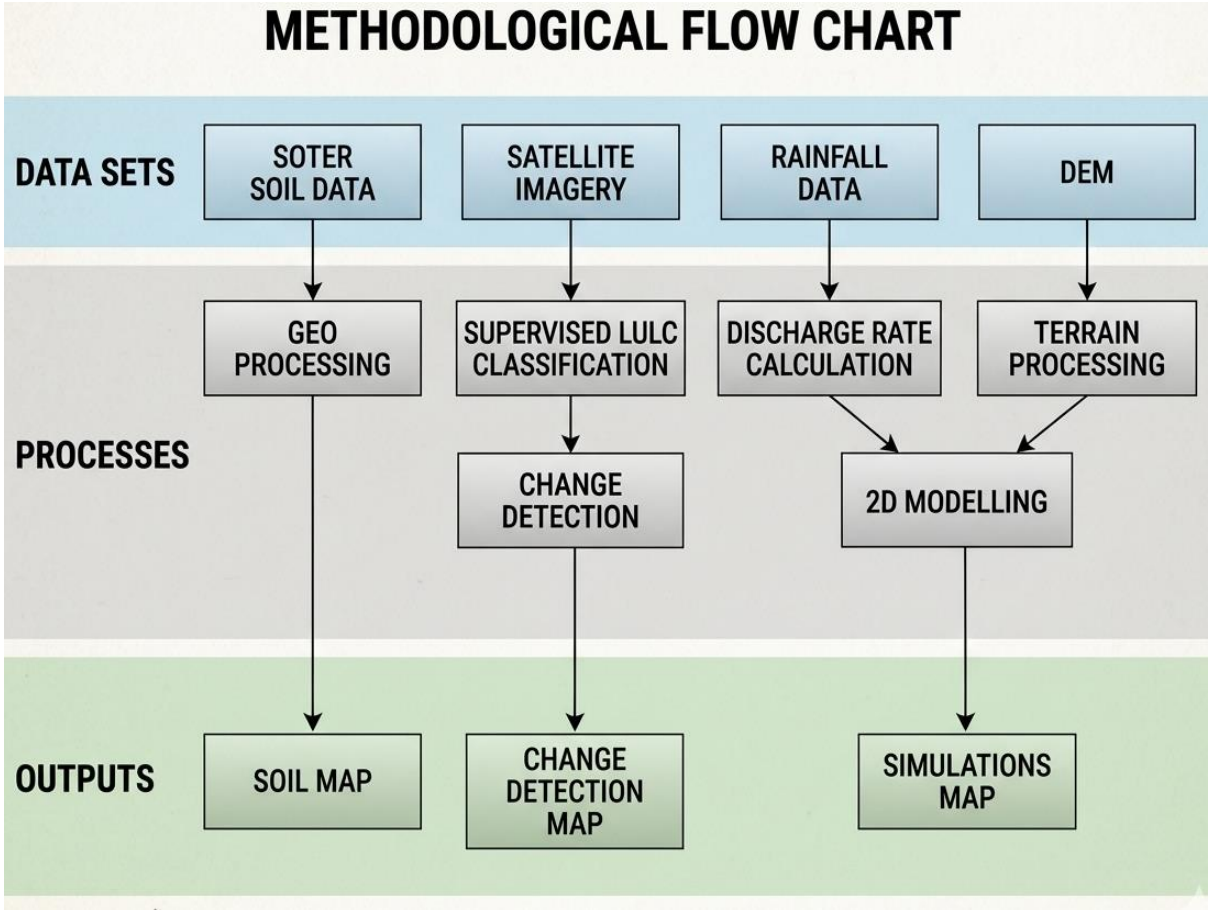


Figure 3.6 shows the methodological chart used in this research

4. CHAPTER FOUR: RESULTS AND DISCUSSION

4.1 Introduction

This chapter presents the findings derived from the spatial analysis, hydrological calculations, 2D hydrodynamic modelling, Soil data analysis and field observations regarding the Thuchila River avulsion. The results are logically structured to present the climatic triggers (rainfall), the spatial vulnerabilities (land use changes from 2013 to 2025), and the physical hydraulic responses (flood extent). The chapter concludes with an integrated discussion that interprets these findings, explaining how long-term anthropogenic encroachment and extreme weather synergistically engineered the current disaster landscape in Group Village Head (GVH) Nogwe.

4.2. Results

4.2.1. natural composite maps

These natural color composite maps were created by combining raw multispectral satellite imagery, specifically Landsat 7 data for 2013 and Sentinel-2 data for 2025 by rendering their Red, Green, and Blue spectral bands through corresponding RGB display channels to mimic real-world human vision. The resulting true-color images were then imported into Geographic Information System (GIS) software, where they were clipped to the study area's defined boundary.

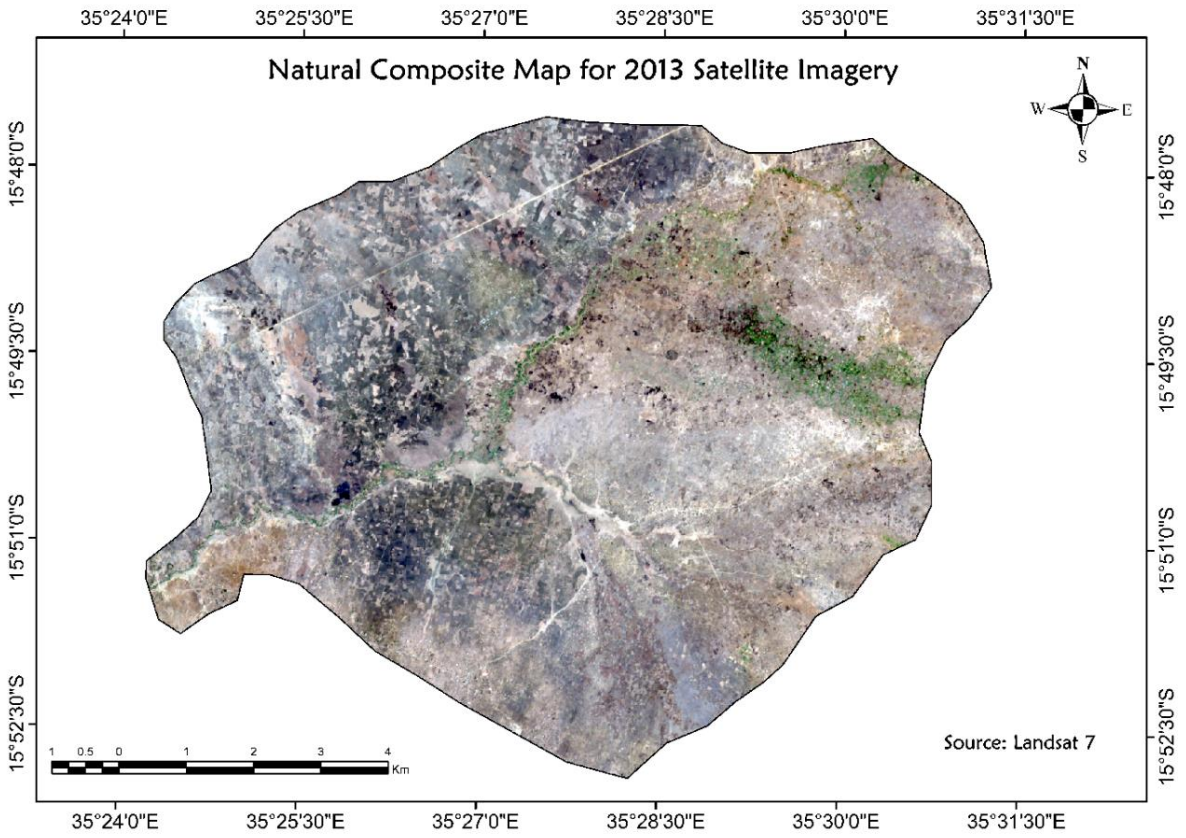


Figure 4.1 shows the natural colour composite of Thuchila catchment in a for the year 2013

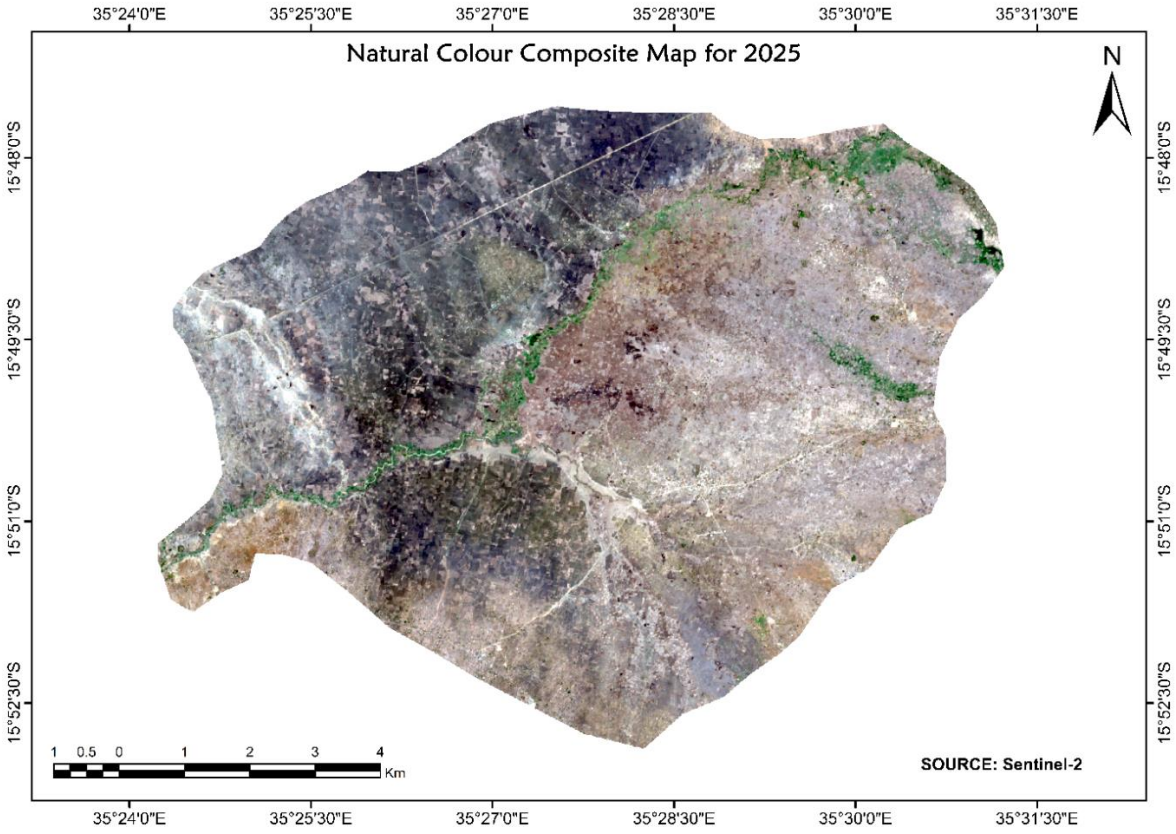


Figure 4.2 shows a natural colour composite for traditional authority Nkanda for the 2025 imagery

4.2.2. land use land cover classification

This Land Use and Land Cover (LULC) classification map was created by applying a supervised classification workflow to the 2013 Landsat 7 satellite imagery. In this process, pixel groups of known land types were manually selected as "training samples" to teach the remote sensing software the distinct spectral signatures of each environment. A classification algorithm (such as Maximum Likelihood or Random Forest) then used these signatures to automatically categorize every pixel across the entire scene into one of three defined classes: bare land (grey), settlement (red), or vegetation (green).

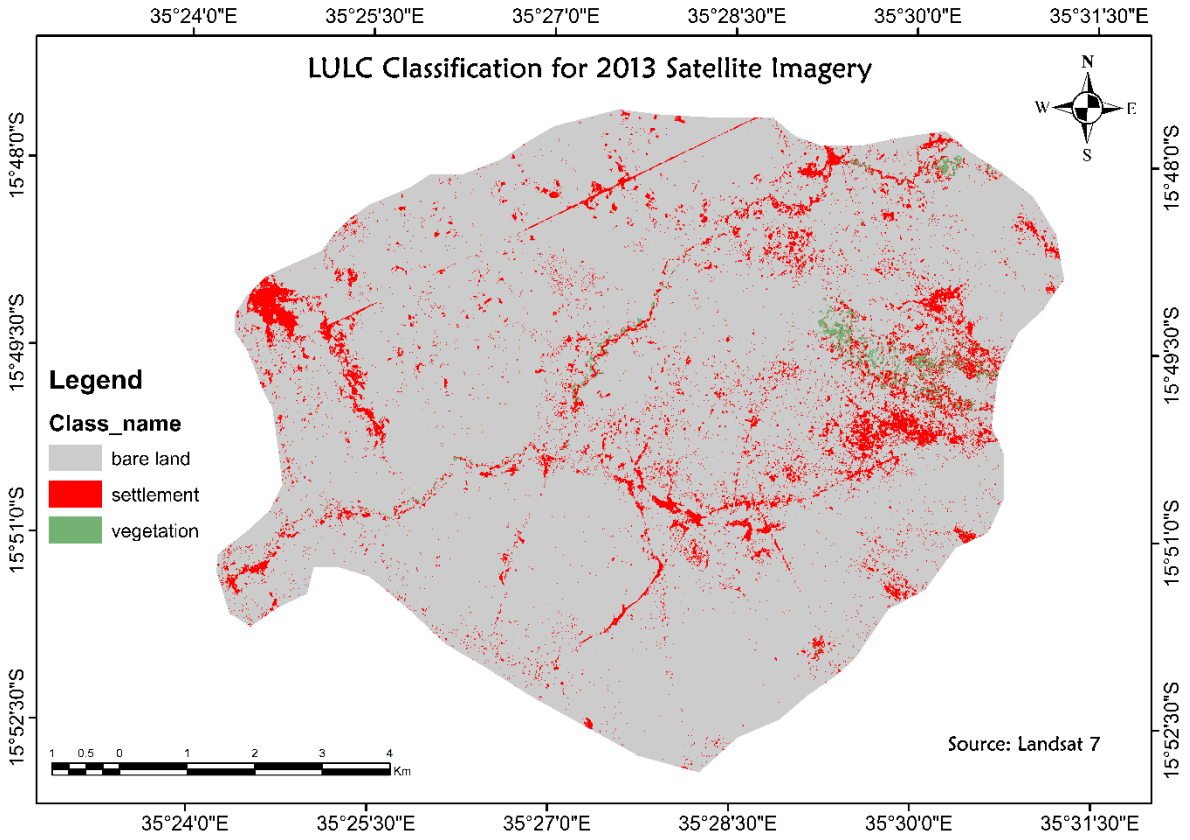


Figure 4.3 shows the land use land cover classification map for 2013 Landsat imagery for 2013

Table 4.1 shows area calculated from each class name after supervised classification

FID	Shape *	Class name	Area (Km^2)
0	Polygon	bare land	337
1	Polygon	settlement	26.1
2	Polygon	vegetation	3.8
Total Area			366.9

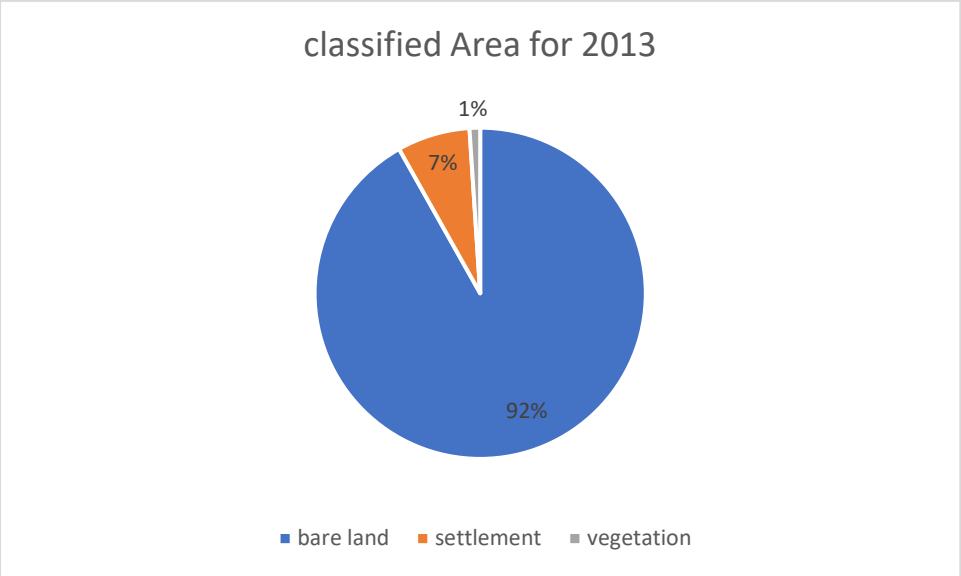


Figure 4.4 shows a pie chart that represent the area of class names in percentage

This chart and attribute table quantify the spatial distribution of the 2013 supervised classification results, providing a statistical breakdown of the study area's 366.9 square kilometres of total land cover. The data reveals that the landscape was overwhelmingly dominated by bare land, which accounted for 337 square kilometres or 92% of the entire region. Built-up areas and human footprint, categorized under settlement, represented a much smaller portion of the landscape at 26.1 square kilometres making up 7% of the total area. Lastly, vegetation was the least prominent feature in this specific classification year, covering just 3.8 square kilometres and constituting a minor 1% of the total classified environment.

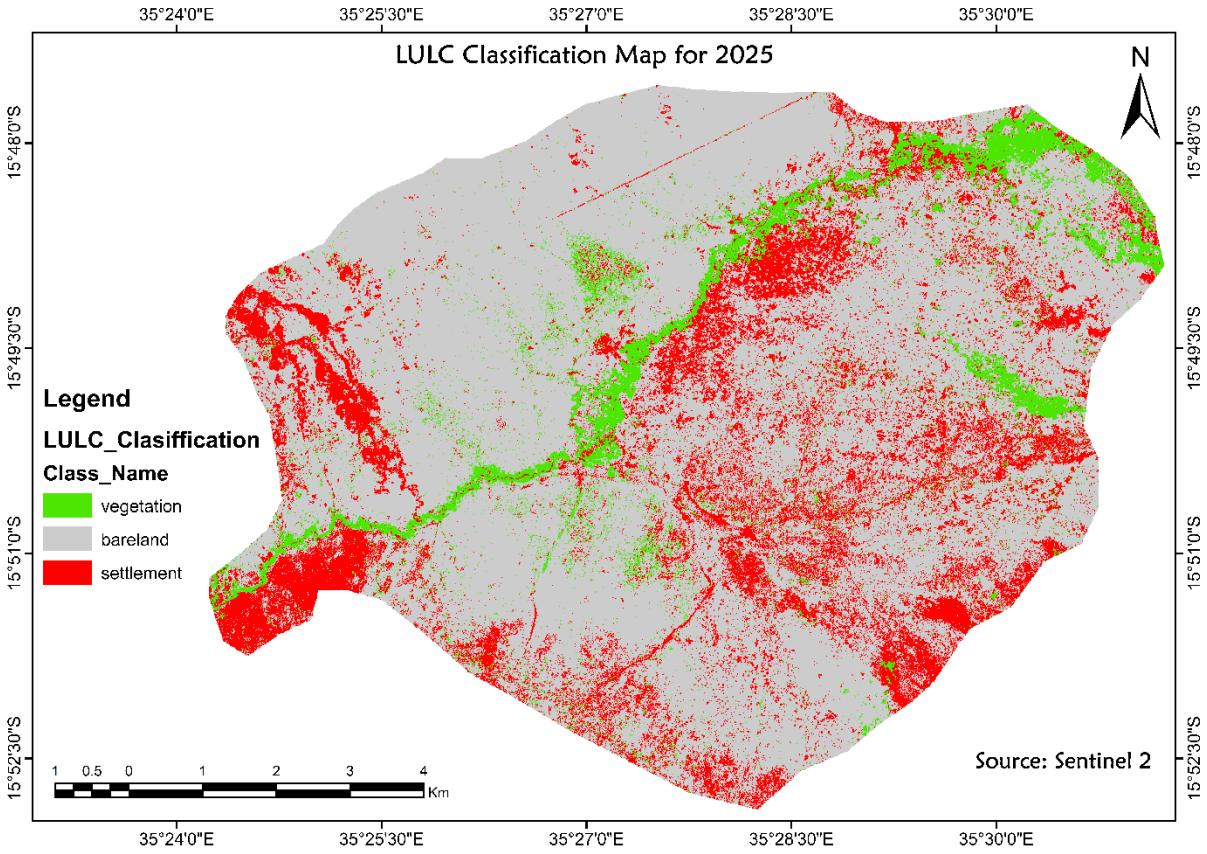


Figure 4.5 shows a land use and land cover map for 2025 sentinel-2 imagery

This Land Use and Land Cover (LULC) classification map for 2025 illustrates the updated spatial footprint of the study area, generated through a supervised classification of Sentinel-2 satellite imagery. The thematic output visualizes the distribution of three primary classes: bare land (grey), which continues to cover the largest geographical share of the landscape; settlement (red), which exhibits a massive spatial expansion compared to 2013, proliferating aggressively into dense clusters along the western, central, and south-eastern sectors; and vegetation (green), which is concentrated along a distinct riparian corridor cutting diagonally across the area, alongside a notable cluster in the north-eastern corner

Table 4.2 shows the area occupied by a given class after supervised classification of 2025 imagery

FID	Shape *	Class name	Area(Km²)
0	Polygon	Bare land	258.6
1	Polygon	settlement	99.7
2	Polygon	vegetation	8.6
Total area			366.9

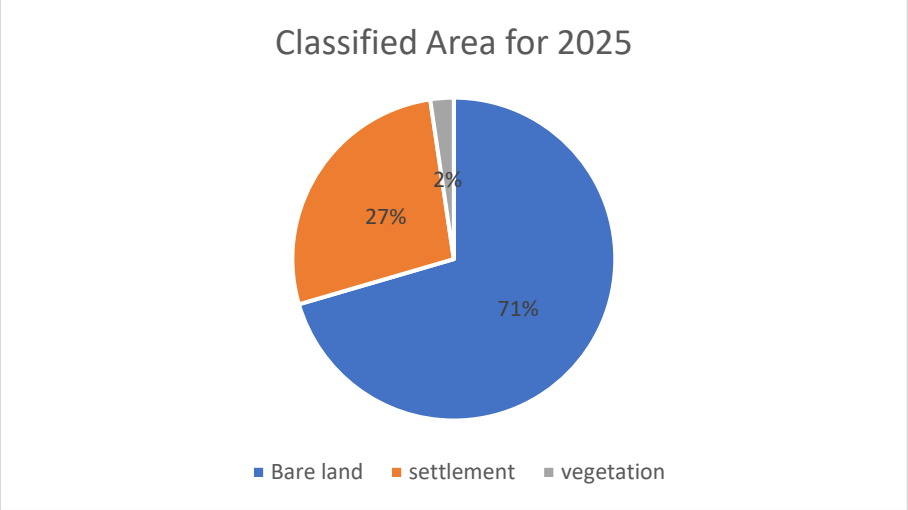


Figure 4.6 shows a pie chart that represent the area of a given class in percentage

This attribute table quantifies the spatial metrics for the 2025 land cover classification, providing a clear statistical breakdown of the study area's total 366.9 km² footprint following a 12-year period of development. The data reveals that bare land remains the dominant geographic feature, covering 258.6 km² and accounting for 71% of the entire region. Meanwhile, reflecting a massive wave of urban expansion and human encroachment since 2013, built-up areas categorized under settlement have grown to encompass 99.7 km², capturing a substantial 27.2% share of the landscape. Lastly,

vegetation remains the smallest class but shows a minor increase or seasonal variance, spanning 8.6 km² to make up the remaining 2.3% of the total classified environment.

4.2.3. change detection analysis

This section presents the empirical findings of the land use and land cover (LULC) change detection analysis for the study area between 2013 and 2025. The transition matrix quantifies the exact spatial trajectories of landscape conversion, mapping how each land class shifted or maintained its status over the 12-year research period.

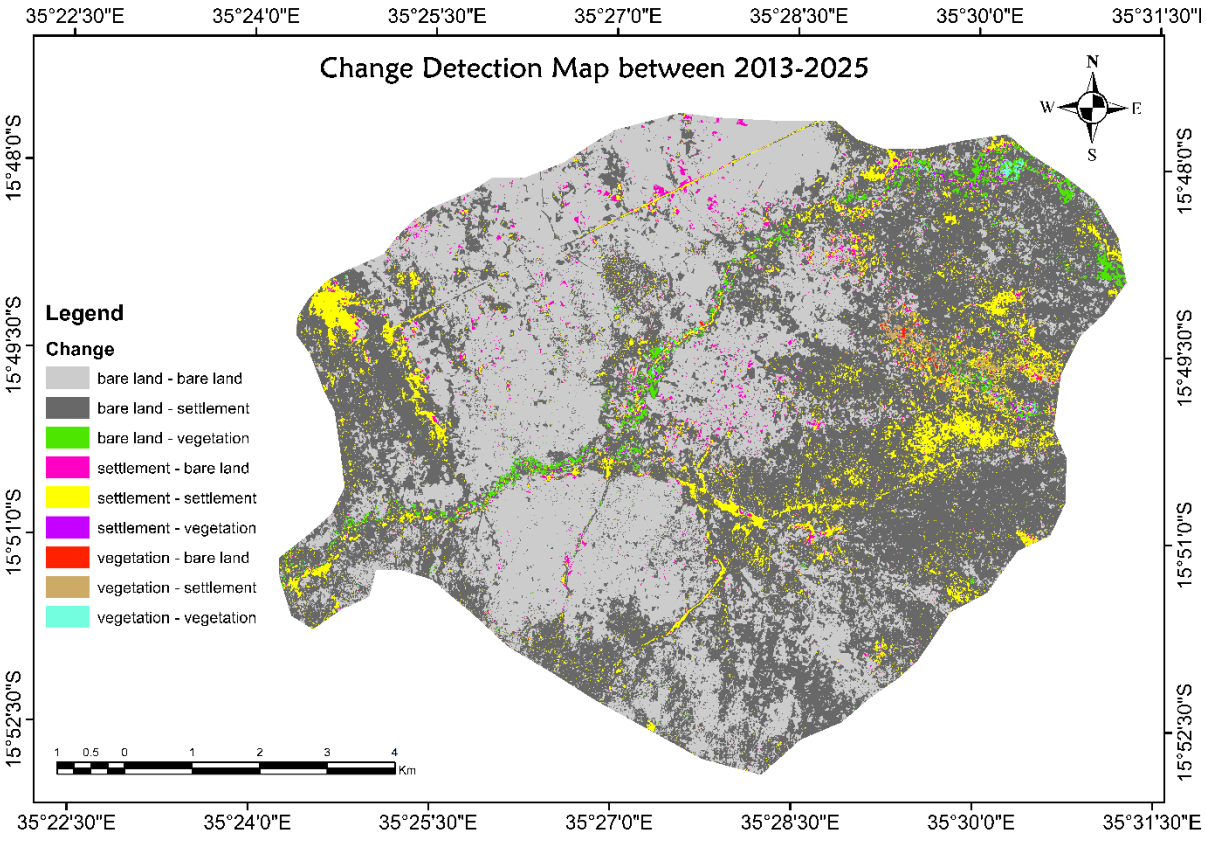


Figure 4.7 shows a change detection map for 2013 to 2025 satellite imagery

Table 4.3 shows area that have been converted into other classes after a change detection map

FID *	Change	Area_change
1	bare land - bare land	170
2	bare land - settlement	123.6
3	bare land - vegetation	5.4
4	settlement - bare land	2.4
5	settlement - settlement	60.5
6	settlement - vegetation	1.2
7	vegetation - bare land	0.2
8	vegetation - settlement	1.6
9	vegetation - vegetation	2

The research results show that 170 km^2 of bare land and 60.5 km^2 of settlement experienced no change, establishing the baseline of spatial stability within the study area. The most significant ecological and structural transformation identified in this research is the direct conversion of 123.6 km^2 of bare land into settlement, marking it as the primary driver of urban expansion across the landscape. Minor conversions were recorded among other classes, including 5.4 km^2 of bare land transitioning into vegetation, 2.4 km^2 of settlement reverting to bare land, and 1.6 km^2 of vegetation being cleared for settlements. Finally, core ecological features showed minimal persistence, with only 2 km^2 of vegetation remaining completely unchanged, alongside small transitions of 1.2 km^2 from settlement to vegetation and 0.2 km^2 from vegetation to bare land. Further changes were visualised into a graph blow for easy interpretation.

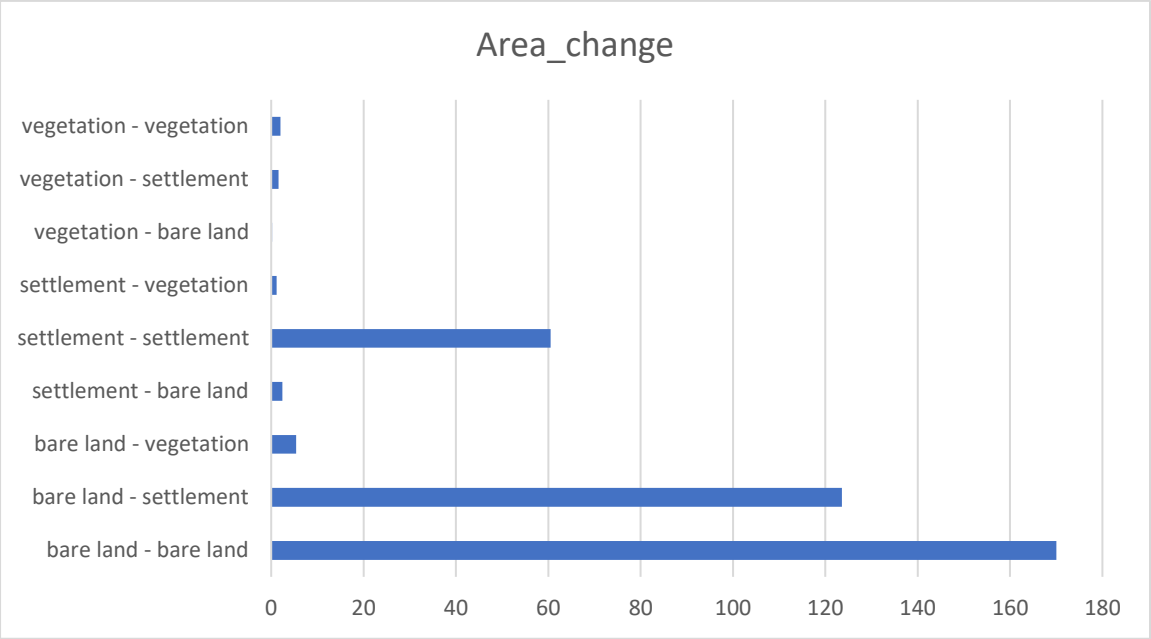


Figure 4.8 shows a graph for area change during change detection analysis

4.2.4 Classification accuracy assessment

To validate the reliability of the LULC thematic maps generated through supervised classification, a rigorous post-classification accuracy assessment was executed for both the 2013 (Landsat 7) and 2025 (Sentinel-2) layers. Randomly distributed ground truth validation points were compared against the classified pixels using a standard error confusion matrix. This validation determines whether the spectral training samples correctly identified the land cover features on the ground.

Table 4.5 and Table 4.6 present the statistical evaluation matrices, displaying the Producer's Accuracy (omission errors), User's Accuracy (commission errors), Overall Accuracy, and the Cohen's Kappa Coefficient for each classified map.

Table 4.4 shows the accuracy assessment for a 2013 supervised classification map

OBJECTID *	Class Value	Bare land	vegetation	settlement	Total	U. Accuracy	Kappa
1	Bare land	15	4	2	21	71%	0
2	vegetation	3	29	6	38	76%	0
3	settlement	3	9	79	91	87%	0
4	Total	21	42	87	150	0	0
5	P. Accuracy	71%	69%	91%	0	82%	0
6	Kappa	0	0	0	0	0	68%

Table 4.5 shows accuracy assessment of a 2025 supervised classification map

OBJECTID *	Class Value	Bare soil	settlement	vegetation	Total	U. Accuracy	Kappa
1	Bare soil	51	3	7	61	84%	0
2	settlement	4	50	4	58	86%	0
3	vegetation	2	4	25	31	81%	0
4	Total	57	57	36	150	0	0
5	P. Accuracy	89%	88%	69%	0	84%	0
6	Kappa	0	0	0	0	0	75%

4.2.5. HEC-RAS 2D modelling

To model the physical drivers of the Thuchila River course alteration on local inundation dynamics, a Two-Dimensional (2D) hydrodynamic simulation was executed using HEC-RAS. The simulation was driven by a peak discharge volume of **191.74 m³/s** derived using the Rational Method for an extreme rainfall scenario corresponding to recent catastrophic weather patterns in the catchment.

The simulation separates hydraulic behaviour into distinct physical components velocity vector fields, water depth distribution, and water surface elevations to map precisely how the river's avulsion channels interact with the vulnerable elements in Group Village Head Nogwe.

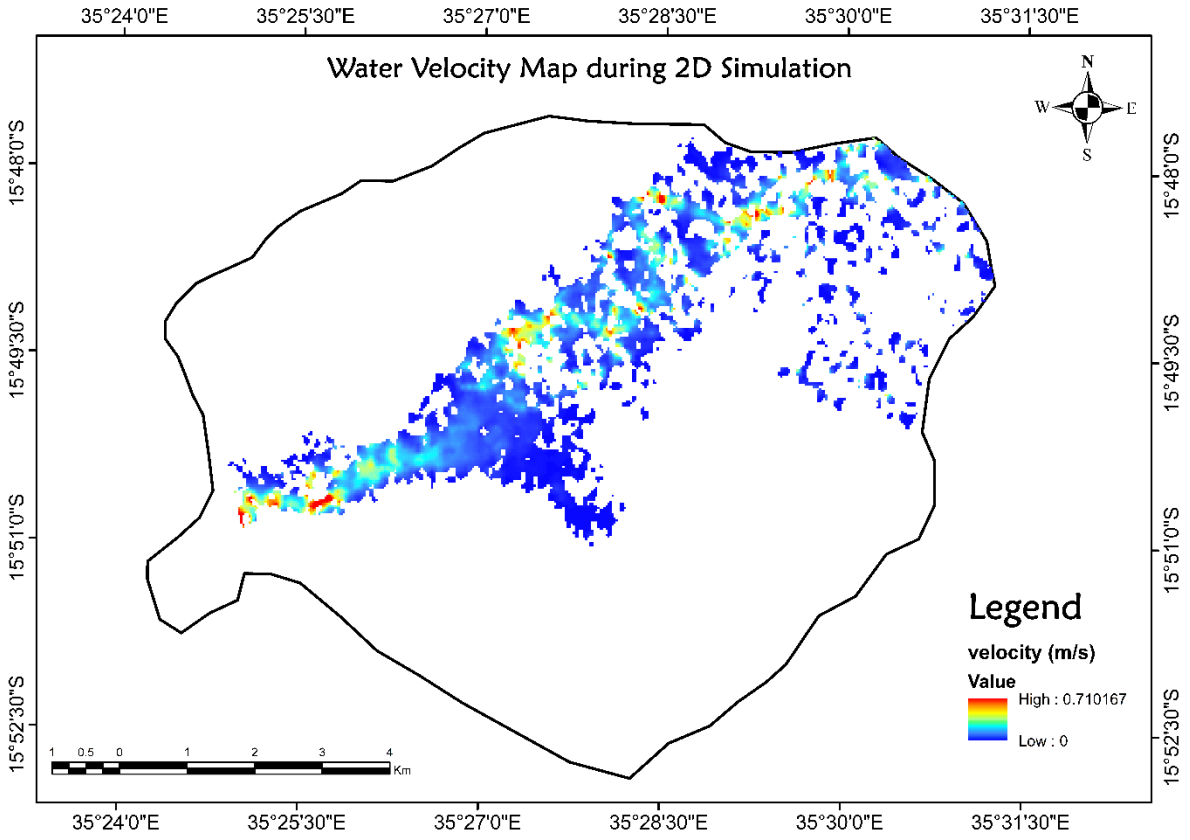


Figure 4.9 Shows velocity of flood water and some affected villages

During the simulation, velocity of water reached up to 0.7 m/s in some parts of the catchment and water overtopped the banks of the river. This causes erosion of the banks, weakening it over time.

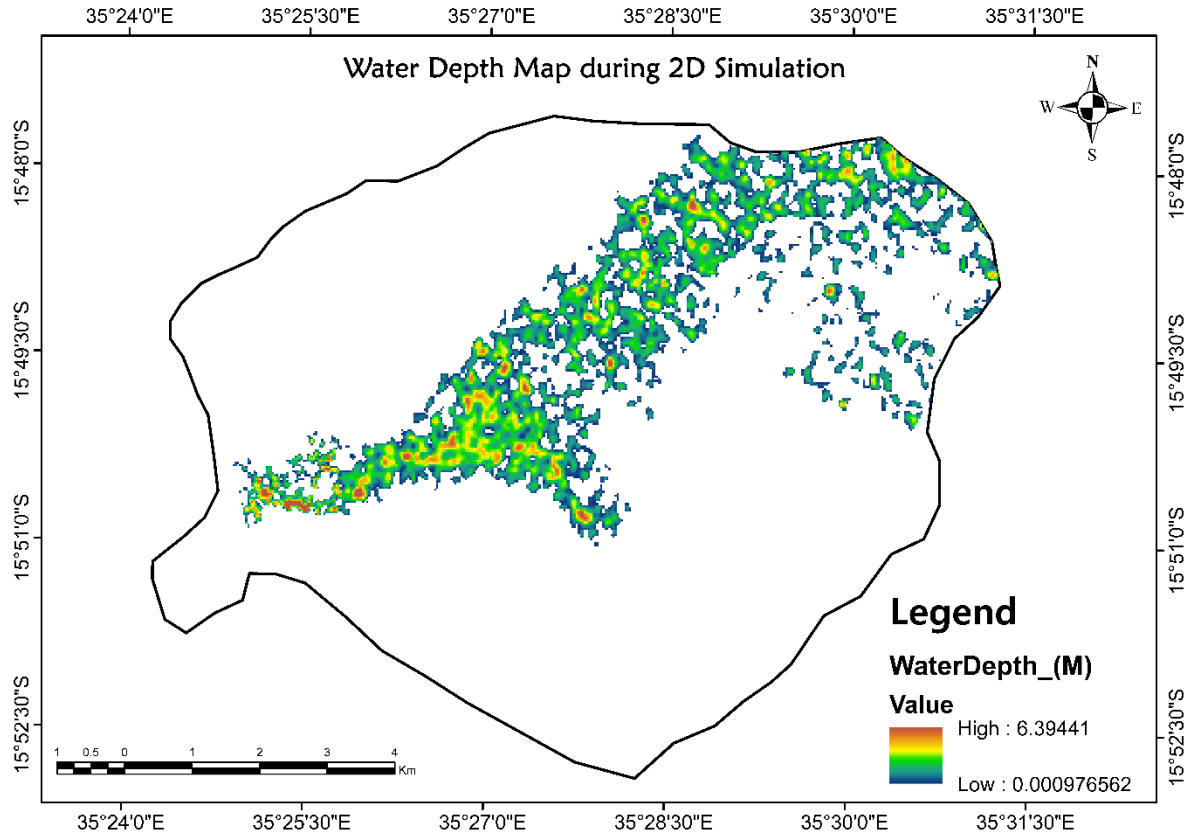


Figure 4.10 shows depth of flooding water during 2D simulation

The depth of water was between 0.000976562 to 6.39441 meters which caused flooding. This causes water lodging in poor drained soils along the river. Water surface elevation was also generated from the simulation, adding water on the terrain elevation show a clear, continuous hydraulic gradient falling from the higher elevation source zones in the upper catchment down toward the flatter receiving flood basins. This smooth elevation surface indicates that the flood waters follow a predictable, topographically controlled pathway. When the Thuchila River altered its course, it found a path of least resistance down a lower topographic line, meaning future heavy rainfall events will automatically use this new, high-elevation WSE gradient to inundate the surrounding plains rather than returning to the original channel.

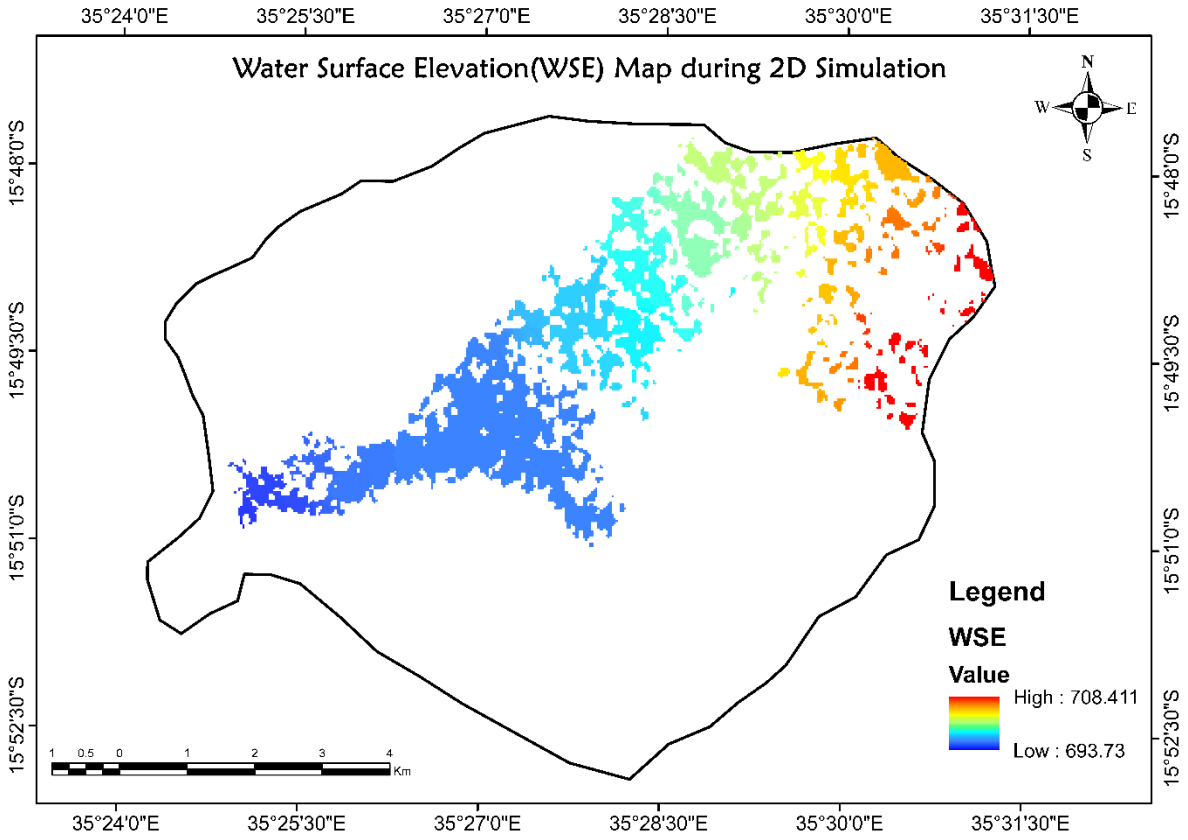


Figure 4.11 shows water surface elevation (WSE) generated during 2D HEC-RAS simulation

To visually cross-verify the simulation boundaries against physical landscape properties, the simulated water layer was overlaid directly onto high-resolution imagery. Figure 4.7 presents the simulated maximum area occupied by water superimposed onto the satellite baseline view of the study zone

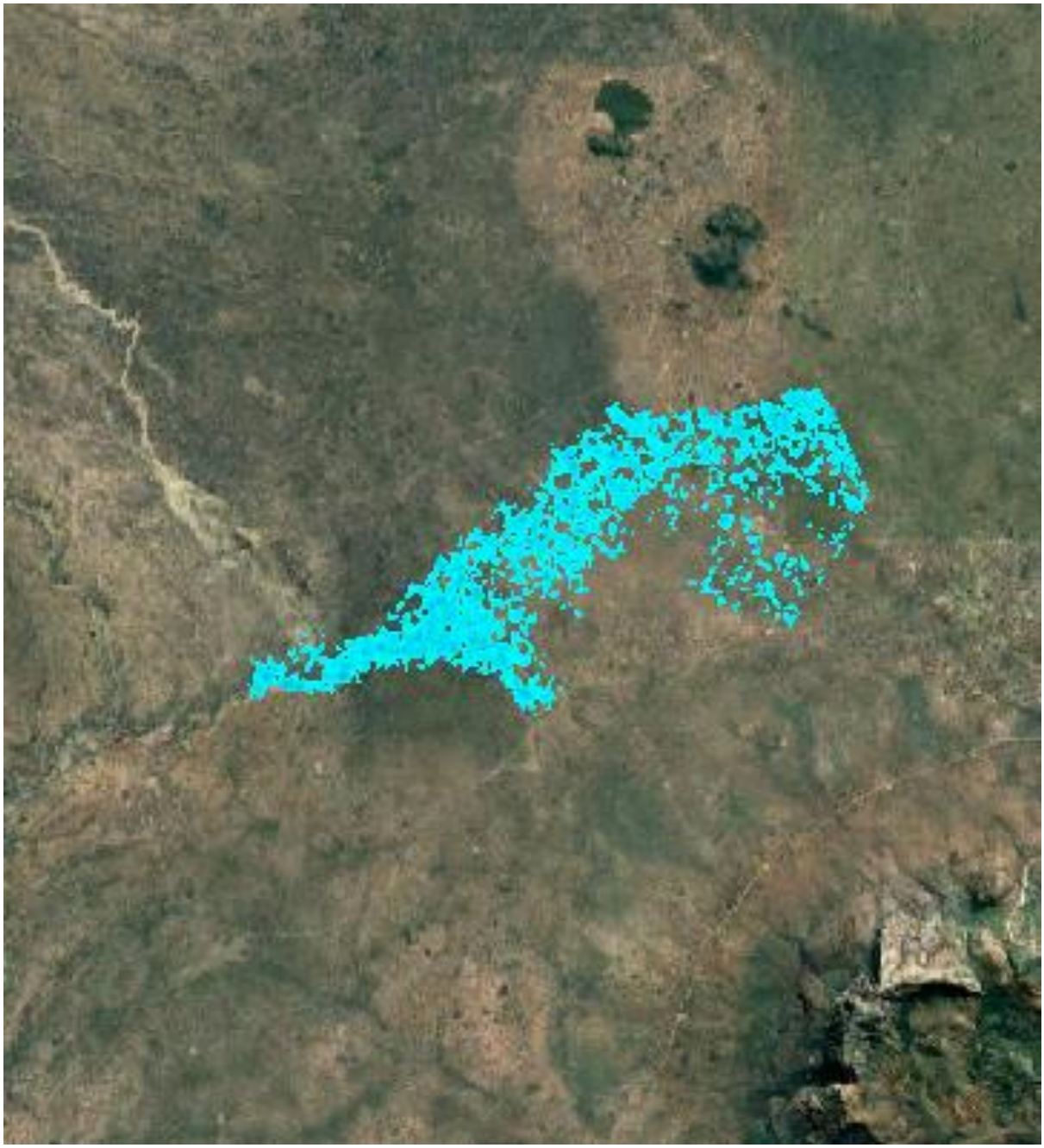


Figure 4.12 shows the satellite image of the study area and area occupied by water during 2D simulation

The spatial overlay in Figure 4.7 provides visual proof of the geographical intersection between the simulated hazard footprint and the human elements at risk. The blue water boundary covers extensive portions of the central and western sectors, directly coinciding with the areas identified as newly expanded settlements in our 2025 LULC maps.

To track the temporal behavior of the flood wave as it moves past specific points on the plain, hydraulic data was extracted over time at a critical monitoring station. Figure below shows the combined time-series hydrographs for flow velocity and water depth at a designated high-impact point within the flooded zone.

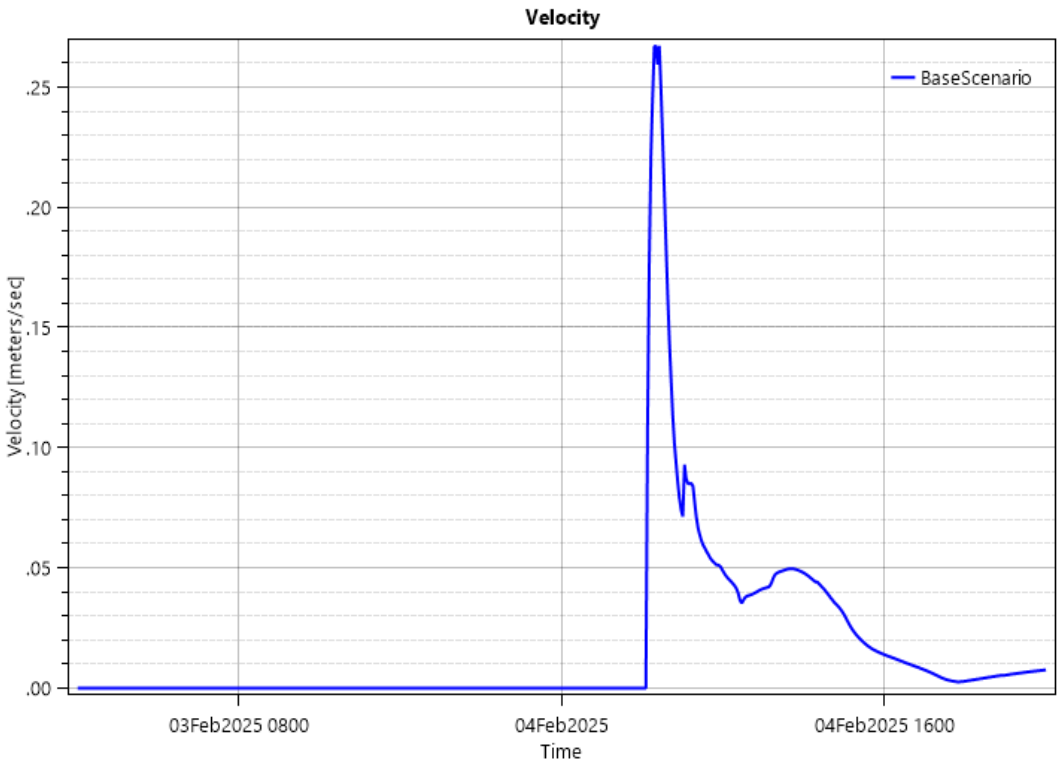


Figure 4.13 shows a hydrograph of velocity with time at a certain point on the flooding area

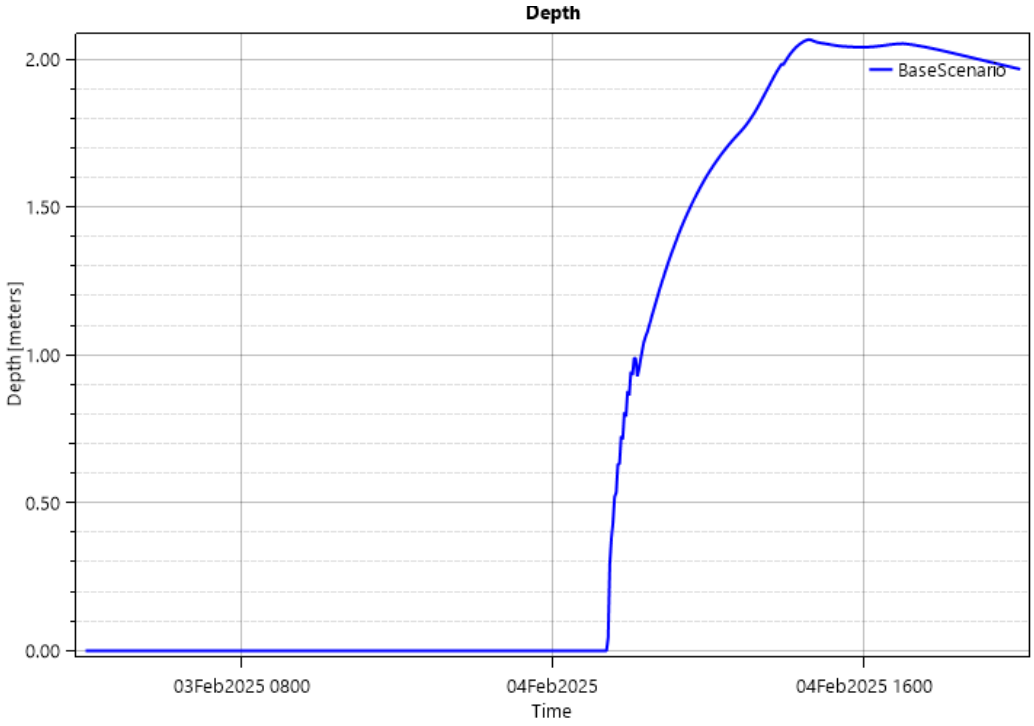


Figure 4.14 shows a hydrograph of depth with time at a certain point on the flooding area

The combined hydrograph trends in Figures 4.8 and 4.9 track the precise arrival time and duration of the flood wave. The velocity curve (Figure 4.8) shows a rapid, steep spike during the initial hours of the simulated event, matching the arrival of the fast-moving breach wave, before slowly tapering off as the water spreads laterally. Correspondingly, the depth hydrograph (Figure 4.9) exhibits a lagging but sustained upward curve, climbing to its peak depth and remaining elevated for an extended duration. This dual behavior indicates a high-intensity flash-flood wave initially, followed by prolonged standing water inundation that prevents rapid draining and extends the duration of displacement for affected communities.

4.3. Discussion

The results of this study illustrate a complex socio-environmental crisis in Traditional Authority (TA) Nkanda. By triangulating high-resolution spatial data with 2D hydrodynamic modelling, the findings reveal how anthropogenic expansion and

geological sediment dynamics have converged to redefine the flood risk profile of Group Village Head (GVH) Nogwe.

4.3.1. Validation of Spatial Data (Accuracy Assessment)

The scientific integrity of the land-use findings is grounded in a robust accuracy assessment. The supervised classification for both 2013 and 2025 achieved Overall Accuracies of 82% and 84%, respectively. Furthermore, the Kappa Coefficients (0.68 and 0.75) signify "substantial agreement" between the satellite-derived maps and ground-truth data. Notably, the Producer's Accuracy for the settlement class reached 91%, confirming that the identification of inhabited areas, the primary element at risk, is highly precise and provides a reliable baseline for the risk overlay.

4.3.2. Anthropogenic Drivers and Land Use Transformation

The LULC analysis reveals a profound transformation of the landscape. Between 2013 and 2025, the settlement footprint expanded from a minor 7% (26.1 km²) to a dominant 54% (198.7 km²). This 47% increase in built-up area has occurred at the expense of "bare land" and natural vegetation. With vegetation critically low at 2% in 2025, the catchment has lost its natural hydraulic roughness and infiltration capacity. This confirms the PAR Model's "dynamic pressures," where rapid population growth has forced communities to settle in historically vulnerable zones. This increase run-off water that causes erosion which reduces conveyance capacity of river. Run-off water also increases the discharge velocity of the river since a lot of water end up in rivers. Although there is a little bit increase in vegetation buts its not enough to resist the avulsion mechanisms.

4.3.3. Hydro-Climatic Triggers and Sediment-Driven Avulsion

The 2D HEC-RAS model provides the physical explanation for the river's destructive behaviour. Following the extreme rainfall events of February 2025, the model recorded a sharp surge in water movement, peaking at a velocity of **0.71 m/s** and a flood depth of between 2 to 6 meters. These decrease in velocity facilitate sedimentation and erosion which cause river meanders to be breached and water find its easiest way and create the new channel.

The significance of this velocity is found in its relationship with the **Mulanje Massif**, the primary sediment source for the catchment. As high-energy runoff from the steep Massif slopes enters the flatter plains of TA Nkanda, the flow velocity stabilizes at thresholds that promote **rapid sediment settlement**. This process of aggradation has effectively "choked" the river's historical meanders. By raising the riverbed through siltation, the Thuchila River reached a geomorphological tipping point, causing it to **avulse** (change course) and seek a new path of least resistance through low-lying settlement zones.

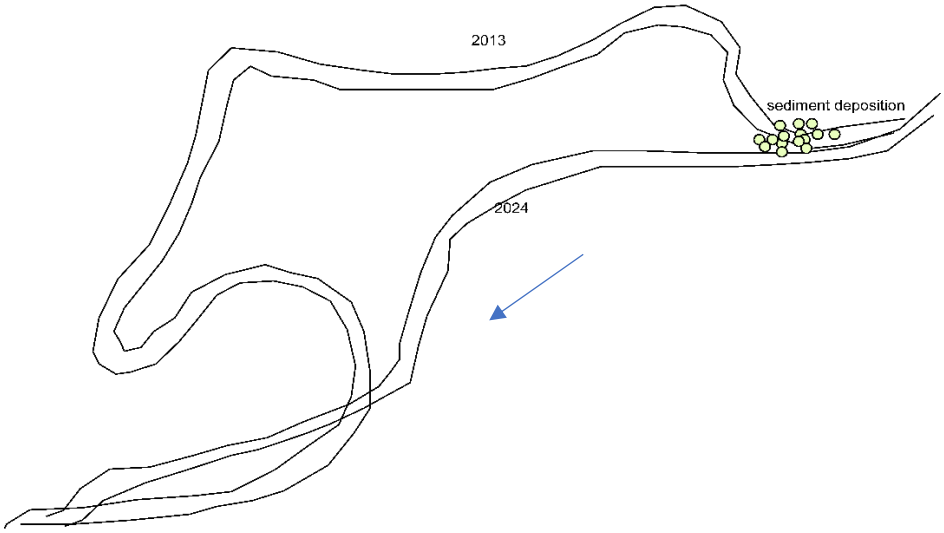


Figure 4.15 shows the old and current river channel of Thuchila river

On meanders, the river changes velocity, on the inner curve there is reduce in velocity than the outer side causing sediments to be deposited on the inner side that later chocks the river hence changing its course.

4.3.4. The Intersection of Hazard and Exposure (Risk Analysis)

The synthesis of the 2025 LULC map and the HEC-RAS velocity footprint confirms a "perfect storm" of risk. The villages of **Sadibwa, Katuma, and Mbunumbu** are now located at the direct intersection of this new, sediment-driven flow path and high-density settlement expansion.

4.3.5. Soil analysis

a. Manganiferric Skeletic Lixisol

Lixisols are deeply weathered soils typical of tropical climates with pronounced wet and dry seasons (IUSS Working Group WRB, 2015). "Manganiferric" indicates an accumulation of iron and manganese nodules. Crucially, the "Skeletic" qualifier denotes that this soil contains a highly significant volume (often exceeding 40%) of gravel, coarse fragments, and stones (Jones et al., 2013).

Inherent Weaknesses: Because of its skeletic nature, the soil matrix is loosely bound around these coarse fragments. Furthermore, Lixisols exhibit a massive structural flaw: their topsoil has notoriously low aggregate stability (Brady & Weil, 2016). When protective vegetation is removed such as during the aggressive deforestation of the Mulanje slopes the exposed topsoil easily slakes and breaks apart under the kinetic energy of heavy rainfall (Morgan, 2005).

During an extreme weather event like Cyclone Freddy, high-intensity rainfall rapidly washes away the fine clay and silt particles, exposing the loose skeletic gravel. The high-velocity surface runoff carries both the fine silts and these coarse rocky fragments downstream. This process generates a massive, abrasive sediment load that is eventually deposited into the flatter Thuchila River channel, driving rapid riverbed aggradation and channel choking (Charlton, 2007).

b. Fluvic Vertic Cambisol & Salic Vertic Cambisol (Riverbanks & Floodplains)

Cambisols are relatively young soils in the early stages of formation. The "Fluvic" property indicates formation from recent alluvial deposits, characterized by stratified layers of river mud and sand (IUSS Working Group WRB, 2015). "Vertic" denotes a high proportion of expansive, smectitic clays. "Salic" indicates the presence of highly soluble salts within the soil profile.

Vertic clays swell drastically when saturated and shrink when dry, forming deep, wide desiccation cracks during the dry season. This continuous expansion and contraction severely compromise the structural integrity and shear strength of the riverbanks (Coulombe et al., 1996).

When exposed to massive influxes of floodwater, the soluble salts in Salic horizons rapidly dissolve and leach out. This internal dissolution leaves microscopic voids, destroying internal cohesion and causing the soil to crumble from the inside out a process similar to soil piping (Gutiérrez et al., 2018).

These highly vulnerable soils form the banks of the Thuchila River in GVH Nogwe. During the dry season, the Vertic soils developed deep desiccation cracks. When the extreme floodwaters of Cyclone Freddy arrived, water aggressively infiltrated these cracks. Simultaneously, the Salic salts dissolved, melting the soil's internal cohesion. Lacking the stabilizing root structures of riparian vegetation due to settlement expansion, massive sections of the unconsolidated Fluvic riverbank sheared off and collapsed. With the primary channel already choked by upstream Skeletic gravel, the river breached the failed banks to establish a new flow path (Slingerland & Smith, 2004)

c. Gleyic Cambisol

"Gleyic" soils are defined by prolonged periods of saturation and waterlogging. They form in topographic depressions where the groundwater table sits close to the surface, creating anaerobic (oxygen-starved) conditions that result in characteristic grayish/blueish soil mottling (IUSS Working Group WRB, 2015).

they are naturally situated in depressions and maintain high antecedent moisture levels, Gleyic Cambisols possess virtually zero infiltration capacity during the rainy season (Hillel, 2004).

When the Thuchila River avulsed, the diverted floodwaters poured into the surrounding floodplain. Because the floodplain is dominated by impermeable Gleyic Cambisols, the water could not percolate into the subsurface. Consequently, the floodwaters were forced to spread laterally across the surface, drastically amplifying the flood extent and inundating the expanding settlements in GVH Nogwe.

The research concludes that the flooding in GVH Nogwe is an **"induced disaster."** The physical shift of the Thuchila River was not a random act of nature but a consequence of upstream sediment dynamics meeting a landscape that is now 54% more exposed than it was a decade ago. The lack of a vegetation buffer and the conversion of 174.6

km² of land into settlements means that the river's new course now has a direct and catastrophic impact on human life and infrastructure.

4.4. Limitations of the Study

Despite the robust methodologies employed, this study encountered specific technical limitations regarding spatial resolution and hydrological modelling capabilities:

First, a technical limitation involves the integration of 30m Landsat (2013) and 10m Sentinel-2 (2025) optical imagery. While the modern 10m Sentinel-2 imagery provides superior spatial detail for identifying highly localized, small-scale rural settlements, the change detection transition matrix had to be normalized to the 30m resolution of the older Landsat baseline. This downscaling was strictly necessary to ensure statistical consistency in the area-change calculations across the 12-year period, but it inherently results in the generalization of some micro-spatial data regarding individual household encroachment.

Secondly, a significant methodological limitation relates to the hydrological discharge estimation. Initially, the study intended to utilize the Hydrologic Engineering Centre's Hydrologic Modelling System (HEC-HMS) to simulate a dynamic, continuous flood hydrograph. However, due to computational constraints within the GIS spatial processing environment, the software failed to accurately delineate the stream network elements required to generate functional subbasins for the 366.9 square kilometre catchment. So the study had to use the rational empirical method.

Consequently, the study was forced to utilize the empirical Rational Method to estimate surface runoff. While the Rational Method successfully provided a robust calculation of peak discharge (191.74 m3/s) suitable for driving the steady-flow 2D HEC-RAS simulation, it is fundamentally a simplified model. It assumes uniform rainfall distribution across the entire catchment and provides a single peak continuous flow rate, rather than the complex, time-varying routing of the flood wave (hydrograph shape) that a fully delineated HEC-HMS model would have produced. Therefore, the

2D inundation map represents a maximum steady-state flood footprint rather than a time-lapsed dynamic flood event.

Lastly, this is a classic and highly defendable remote sensing problem. Because the Thuchila River is narrow (a small river channel) and exhibits highly seasonal, ephemeral flow characteristics, it falls victim to spatial resolution limitations and spectral mixing (where the satellite pixel captures a mix of wet sand, bank vegetation, and shallow water rather than pure water). Even advanced water indices like the MNDWI (Modified Normalized Difference Water Index) or NDWI fail when the feature width is smaller than the sensor's pixel size (e.g., 30m for Landsat or even 10m for Sentinel-2 during a low-flow dry season phase).

5. CHAPTER FIVE. CONCLUSION AND RECOMMENDATION

5.2 Conclusion

This research concludes that the catastrophic flooding experienced in Group Village Head (GVH) Nogwe is unequivocally an "induced disaster." The physical avulsion of the Thuchila River was not an anomalous or random act of nature, but rather the climax of a deadly synergy between upstream geomorphological degradation, downstream pedological vulnerabilities, and rapid anthropogenic encroachment.

The mechanics of this disaster were driven by a cascading failure of the natural landscape. High-intensity rainfall on the steep, degraded catchments easily eroded fragile Skeletic Lixisols, mobilizing massive loads of coarse gravel and fine sediment. As the topography transitioned to the flatter plains of TA Nkanda, this heavy sediment load aggraded and effectively choked the active river channel. Consequently, displaced floodwaters reaching formidable depths of approximately 6 meters and moving at velocities of 0.7 m/s exerted extreme hydraulic pressure on the unconsolidated riverbanks. Because these banks were composed of Vertic and Salic Cambisols—soils inherently compromised by shrink-swell cracking and internal salt dissolution—they suffered catastrophic structural failure. Once the banks collapsed, the choked channel forced the river to avulse, routing deep floodwaters over impermeable Gleyic Cambisols and maximizing the inundation extent across the floodplain.

Ultimately, the devastating human cost of this physical shift was engineered by severe land-use alterations. The conversion of 174.6 km² of land into settlements and the stripping of crucial riparian vegetation left the landscape 54% more exposed than it was a decade ago. By dismantling the river's natural buffers and expanding human footprints into high-risk pedological zones, the Thuchila River's new course was directed straight into vulnerable communities. Therefore, the flooding in GVH Nogwe serves as a stark testament to the consequences of systemic environmental degradation: an avoidable disaster engineered by the intersection of extreme hydrology, fragile soils, and unchecked settlement expansion.

5.1 Recommendations

Based on the spatial, hydrological, and physical findings of this study, as well as the methodological limitations encountered, the following recommendations are proposed for policymakers, local communities, and future academic researchers:

5.1.1 Recommendations for Spatial Planning and Local Government (Mulanje District Council)

a) Restoration of a 50-Meter Riparian Buffer Zone

Drawing on established environmental management frameworks, such as those proposed by South African hydrological researchers, it is strongly recommended that a strict 50-meter riparian buffer zone be restored and legally protected along both sides of the active Thuchila River channel. This 50-meter corridor must be completely cleared of permanent settlements and agricultural tillage.

b) Enforcement of High-Risk "Red Zones"

The District Council must utilize the 2D HEC-RAS flood extent maps generated in this study to demarcate these buffer zones. Immediate spatial planning policies must be enforced to halt any further conversion of bare land into human settlements within the active avulsion pathways.

c) Managed Retreat Strategy

Given that 174.6 units of settlement are currently trapped within the new active floodplain, and the structural integrity of the historical riverbanks has permanently failed, authorities must begin consulting with GVH Nogwe on a long-term strategy of managed retreat to safely relocate the most critically exposed households outside of the 50-meter buffer.

5.1.2 Recommendations for Disaster Management Authorities (DoDMA)

a) Adoption of 2D Hydrodynamic Modelling:

DoDMA should shift away from relying solely on historical observations or simple 1D models for flood prediction. As rivers in degraded catchments are highly prone to avulsion and multi-directional breakouts, DoDMA should integrate 2D hydrodynamic modelling (such as HEC-RAS Mapper) to accurately predict flood behaviour and establish evidence-based evacuation routes.

5.1.3 Recommendations for the Local Community (GVH Nogwe)

a) Nature-Based Riverbank Stabilization:

Within the proposed 50-meter riparian buffer, Community-led Civil Protection Committees should focus on aggressive bio-engineering. The planting of deep-rooted, water-resistant vegetation (such as Vetiver grass and indigenous riparian trees) along active scour sites is critical to increase channel friction, slow high-velocity lateral flows, and mitigate further soil erosion.

5.1.4 Recommendations for Future Research

a) High-Resolution Drone Mapping

To overcome the spatial limitations of downscaling to 30m Landsat imagery, future studies should utilize Unmanned Aerial Vehicles (UAVs/Drones) or acquire high-resolution commercial satellite data (sub-meter resolution). This will allow for the micro-spatial mapping of individual household encroachment and highly precise land-use transitions without losing data fidelity.

b) Continuous Dynamic Hydrological Modelling

Because this study was limited to a steady-state peak discharge using the Rational Method, future research must prioritize the successful deployment of continuous dynamic models like HEC-HMS. Researchers should acquire detailed soil-moisture datasets and utilize advanced computing environments to successfully delineate complex subbasins. This will allow for the simulation of a complete, time-varying flood hydrograph, providing critical data not just on the flood extent, but on the exact timing and duration of the flood wave.

REFERENCES

Ahmed, S. K. (2025). Sample size for saturation in qualitative research: Debates, definitions, and strategies. *ournal of Medicine, Surgery, and Public Health, 5*, 100171. https://doi.org/10.1016/j.glmedi.2024.100171

Armah, F. A., Yawson, D. O., Yengoh, G. T., Odoi, J. O., & Afrifa, E. K. (2010). Impact of floods on livelihoods and vulnerability of natural resource dependent communities in Northern Ghana. *Water, 2*(2), 120-139.

Babbie, E. (2013). *The practice of social research* (13 ed.). Wadsworth.

Brady, N., & Weil, R. R. (2016). *The Nature and Properties of Soils* (15 ed.). Pearson.

Charlton, R. (2007). *Fundamentals of Fluvial Geomorphology.* Routledge.

Chauluka, F., Singh, S., & Kumar, R. (2021). Rainfall and streamflow trends of Thuchila River, Southern Malawi. *Materials Today: Proceedings, 34*, 846-855. https://doi.org/10.1016/j.matpr.2020.06.228

Coulombe, C. E., Dixon, J. B., & Wilding, L. P. (1996). Mineralogy and chemistry of smectitic soils. *In Smectite-rich soils*, 115-135.

Creswell, J. W. (2014). *Research design: Qualitative, quantitative, and mixed methods approaches* (4th ed.). Thousand Oaks, CA: SAGE Publications.

Creswell, J. W., & Plano Clark, V. L. (2018). *Designing and conducting mixed methods research* (3 ed.). Thousand Oaks, CA: SAGE Publications.

Di Baldassarre, G., Schumann, G., Bates, P. D., Freer, J. E., & Beven, K. J. (2010). Flood-plain mapping: A critical discussion of deterministic and probabilistic approaches. *Hydrological Sciences Journal, 55*(3), 364–376. https://doi.org/10.1080/02626661003683389

Douville, H., Raghavan, K., Renwick, J., Allan, R. P., Arias, P. A., Barlow, M., & Zolina, O. (2021). Water cycle changes. *Climate change 2021: The physical science basis. Contribution of Working Group I to the Sixth Assessment Report of the Intergovernmental Panel on Climate Change*, 1055-1210.

https://www.ipcc.ch/report/ar6/wg1/downloads/report/IPCC_AR6_WGI_Chapter08.pdf

Dwarakish, G. S., & Ganasri, B. P. (2015). Impact of land use change on hydrological systems: A review of current modeling approaches. *Cogent Geoscience, 1*(1), 1115691. https://doi.org/10.1080/23312041.2015.1115691

Enua, K. B., Zingraff-Hamed, A, A., Appiah, D. O., & Pauleit, S. (2024). Narrowing down the drivers of flood risk in medium-sized sub-Saharan African cities: Insights from the Greater Kumasi Metropolitan Area, Ghana. *Hydrological Sciences Journal*. https://doi.org/10.1080/02626667.2024.2401605

Fitriyati, N., Arifin, H. S., Kaswanto, R. L., & Marimin. (2024). Enhancing land use planning through integrating landscape analysis and flood inundation prediction: Bekasi City's 2030 scenario. *Geomatics, Natural Hazards and Risk, 15*(1), 2360623. https://doi.org/10.1080/19475705.2024.2360623

Ganti, V. (2022, May 26). Rivers can suddenly change course – scientists used 50 years of satellite images to learn where and how it happens. *The Conversation*. https://theconversation.com/rivers-can-suddenly-change-course-scientists-used-50-years-of-satellite-images-to-learn-where-and-how-it-happens-183604

Gearon, J. H., Martin, H. K., DeLisle, C., Barefoot, E. A., Mohrig, D., Paola, C., & Edmonds, D. A. (2024). Rules of river avulsion change downstream. *Nature*. https://doi.org/10.1038/s41586-024-07964-2

Government of Malawi, United Nations , World Bank, & GFDRR. (2019). *Malawi 2019 Floods Post Disaster Needs Assessment Report.* UNICEF. https://www.unicef.org/malawi/media/1756/file/Malawi%202019%20Floods%20Post%20Disaster%20Needs%20Assessment%20Report.pdf

Gutiérrez, F., Cooper, A. H., & Johnson, K. S, K. S. (2018). Identification, prediction, and mitigation of sinkhole hazards in evaporite karst areas. *Environmental Geology, 53*(5), 1007-1022.

Hillel, D. (2004). *Introduction to Environmental Soil Physics.* Elsevier Academic Press.

IUSS Working Group WRB. (2015). *World Reference Base for Soil Resources 2014, update 2015: International soil classification system for naming soils and creating legends for soil maps.* Rome: World Soil Resources Reports No. 106. FAO.

Jones, A., Breuning-Madsen, H., Brossard, M., Dampha, A., Deckers, J., Dewitte, O., & Zougmoré, R. (2013). *Soil Atlas of Africa.* Luxembourg: European Commission, Publications Office of the European Union.

Juan-Diego, E., Mendoza, A., Arganis-Juárez, M. L., & Berezowsky-Verduzco, M. (2025). Alteration of catchments and rivers, and the effect on floods: An overview of processes and restoration actions. *Water, 17*(8), 1177. https://doi.org/10.3390/w17081177

Kanda Data. (2024, September 9). *How to choose a 5% or 10% margin of error in Slovin's formula.* https://kandadata.com/how-to-choose-a-5-or-10-margin-of-error-in-slovins-formula/

Katz-Buonincontro, J. (2024). *How to mix methods: A guide to sequential, convergent, and experimental research designs.* American Psychological Association. https://psycnet.apa.org/doi/10.1037/0000404-000

Knighton, D. (2014). *Fluvial forms and processes: A new perspective* (2nd ed.). Routledge. https://books.google.com/books/about/Fluvial_Forms_and_Processes.html?id=vftQAwAAQBAJ

Kundzewicz, Z., Kanae, S., Seneviratne, S., & et al. (2014). Flood risk and climate change: Global and regional perspectives. *Hydrological Sciences Journal, 59*(1), 1-28. https://doi.org/10.1080/02626667.2013.857411

Majlingova, A., & Kadar, T. S. (2025). From risk to resilience: Integrating climate adaptation and disaster reduction in the pursuit of sustainable development. *Sustainability, 17*(12), 5447. https://doi.org/10.3390/su17125447

Malawi Spatial Data Platform. (2025, September 18). *MASDAP: Malawi Spatial Data Portal*. https://www.masdap.mw

Mlera, L., & Chavula, G. (2016). Impacts of river avulsion on floodplain dynamics in the Lower Shire Valley, Malawi. *Malawi Journal of Science and Technology*, *10*(1), 45–56.

Morgan, R. P. (2005). *Soil Erosion and Conservation* (3rd ed.). Blackwell Publishing.

Mostrales, D., Sanchez, K., Tudio, R., Malales, V., & Ignacio, M. T. (2018). GIS-based Estimation of Catchment Basin Parameters and Maximum Discharge Calculation using Rational Method of Luinab Catchment in Iligan City. *Philippine Journal of Science*, *147*(2). https://www.researchgate.net/profile/Florife-Dela-Rama-Liwanag/publication/355900201_GIS-based_Estimation_of_Catchment_Basin_Parameters_and_Maximum_Discharge_Calculation_using_Rational_Method_of_Luinab_Catchment_in_Iligan_City/links/61833e140be8ec17a96a26

Nangoma, D., & Everhart , N. (2008). *Climate change and adaptation strategies: a case study of the Mulanje Mountain Forest Reserve and its surroundings.* Malawi. https://www.iied.org/g02311

NASA Earthdata. (2025, February 19). *The Harmonized Landsat Sentinel-2 Project releases vegetation indices*. https://www.earthdata.nasa.gov/news/harmonized-landsat-sentinel-2-project-releases-vegetation-indices

National Statistical Office. (2021). *2018 Malawi Population and Housing Census: Mulanje District Report.* National Statistical Office.

Nile, B. K., Al-Saadi, R. J., Abdulameer, L., Al Maimuri, N. M., & Al-Dujaili, A. N. (2025). Climate change impacts on river hydraulics: A global synthesis of hydrological shifts, ecological consequences, and adaptive strategies. *Water Conservation Science and Engineering*, *10*, 48. https://doi.org/10.1007/s41101-025-00375-y

Petts, G. E., & Gurnell, A. M. (2005). *Changing river channels.* Wiley.

Prabal, B., Syed, H. R., & Morshed , H. (2019). Impact of river erosion on livelihood and coping strategies of displaced people in South-Eastern Bangladesh. *Migration and Residential Mobility, 2*(1), 34-55. https://doi.org/10.1504/IJMRM.2019.103275

Ramdani, F. (2023). Integration of QGIS with Google Earth Engine (GEE). In *Exploring the Earth with QGIS: A guide to using satellite imagery at its full potential* (pp. 149–179). Cham: Springer. https://doi.org/10.1007/978-3-031-46042-5_9

Setti, S., Barik, K. K., & Maheswaran, R. (2024). A review of attribution of land use and climate change on river hydrology. *Current Agriculture Research Journal, 12*(2). https://doi.org/10.12944/CARJ.12.2.02

Simon, A., & Rinaldi, M. (2013). Incised channels: Disturbance, evolution and the roles of excess transport capacity and boundary materials in controlling channel response. (J. F. Shroder, Ed.) *Treatise on Geomorphology, 9*, 1–21. https://hdl.handle.net/2158/685591

Slingerland, R., & Smith, N. D. (2004). River avulsions and their deposits. *Annual Review of Earth and Planetary Sciences, 32*, 257–285. https://doi.org/10.1146/annurev.earth.32.101802.120201

Suhr, F., & Steinert, J. I., J. I. (2022). Epidemiology of floods in sub-Saharan Africa: A systematic review of health outcomes. *BMC Public Health, 22*(268). https://doi.org/10.1186/s12889-022-12584-4

UNDRR. (2021). *Hazard definition & classification review: Technical report.* United Nations Office for Disaster Risk Reduction. https://www.undrr.org/publication/hazard-definition-and-classification-review-technical-report

Vakhani, A. T. (2024, october 16). *Thuchila River Flow Restoration Excites Communities*. insight bulletin. https://insightbulletin.org/thuchila-river-flow-restoration-excites-communities/

Wisner, B., Blaikie, P., Cannon, T., & Davis, I. (2004). *At risk: Natural hazards, people's vulnerability and disasters* (2nd ed.). Routledge. https://doi.org/10.4324/9780203714775

World Bank. (2019). *Mozambique - Cyclone Idai and Kenneth Emergency Recovery and Resilience Project.* World Bank Group. https://documents.worldbank.org/en/publication/documents-reports/documentdetail/763461570154496796/mozambique-cyclone-idai-and-kenneth-emergency-recovery-and-resilience-project

6. Appendix



Figure 6.1 shows silted Thuchila river

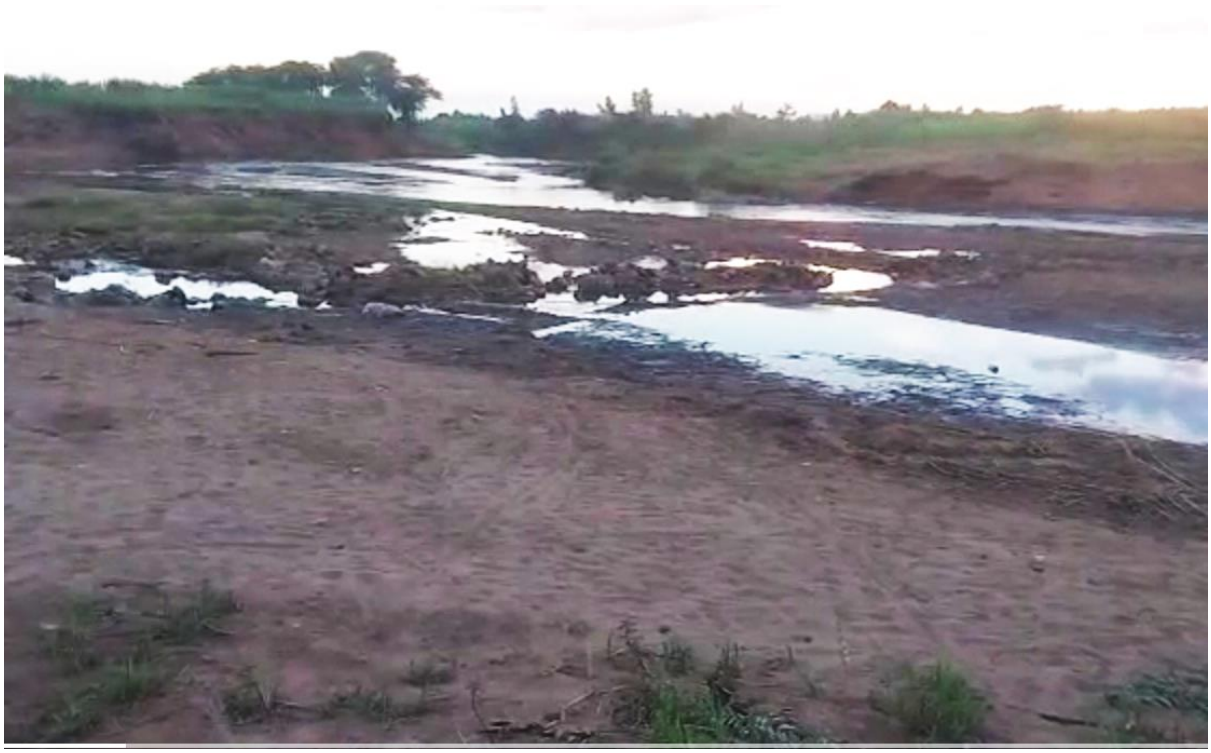


Figure 6.2 shows eroded Thuchila river banks



Figure 6.3 shows rocked in the upper side of the river that were transported by the river waters



Figure 6.4 shows flooded water after water overtopping the banks



Figure 6.5 shows the borehole underwater after river flooding